THE JOURNAL OF BIOLOGICAL CHEMISTRY VOL. 291, NO. 32, pp. 16904–16919, August 5, 2016

20-Hydroxyeicosatetraenoic Acid (HETE)-dependent Hypertension in Human Cytochrome P450 (*CYP*) *4A11* Transgenic Mice

*NORMALIZATION OF BLOOD PRESSURE BY SODIUM RESTRICTION, HYDROCHLOROTHIAZIDE, OR BLOCKADE OF THE TYPE 1 ANGIOTENSIN II RECEPTOR**

Received for publication, April 12, 2016, and in revised form, June 7, 2016 Published, JBC Papers in Press, June 13, 2016, DOI 10.1074/jbc.M116.732297

Üzen Savas[‡], Shouzou Wei[§], Mei-Hui Hsu[‡], John R. Falck[¶], F. Peter Guengerich[‖], Jorge H. Capdevila[§], and Eric F. Johnson[‡1]

From the [‡]Department of Molecular and Experimental Medicine, The Scripps Research Institute, La Jolla, California 92037, the Departments of [§]Medicine and [‖]Biochemistry, Vanderbilt University School of Medicine, Nashville, Tennessee 37232, and the [¶]Department of Biochemistry, The University of Texas Southwestern Medical Center at Dallas, Dallas, Texas 75390

Male and female homozygous 129/Sv mice carrying four copies of the human cytochrome P450 4A11 gene (*CYP4A11*) under control of its native promoter (B-129/Sv-4A11$^{+/+}$) develop hypertension (142 ± 8 *versus* 113 ± 7 mm Hg systolic blood pressure (BP)), and exhibit increased 20-hydroxyeicosatetraenoic acid (20-HETE) in kidney and urine. The hypertension is reversible by a low-sodium diet and by the CYP4A inhibitor HET0016. B-129/Sv-4A11$^{+/+}$ mice display an 18% increase of plasma potassium ($p < 0.02$), but plasma aldosterone, angiotensin II (ANGII), and renin activities are unchanged. This phenotype resembles human genetic disorders with elevated activity of the sodium chloride co-transporter (NCC) and, accordingly, NCC abundance is increased by 50% in transgenic mice, and NCC levels are normalized by HET0016. ANGII is known to increase NCC abundance, and renal mRNA levels of its precursor angiotensinogen are increased 2-fold in B-129/Sv-4A11$^{+/+}$, and blockade of the ANGII receptor type 1 with losartan normalizes BP. A pro-hypertensive role for 20-HETE was implicated by normalization of BP and reversal of renal angiotensin mRNA increases by administration of the 20-HETE antagonists 2-((6*Z*,15*Z*)-20-hydroxyicosa-6,15-dienamido)acetate or (*S*)-2-((6*Z*,15*Z*)-20-hydroxyicosa-6,15-dienamido)succinate. SGK1 expression is also increased in B-129/Sv-4A11$^{+/+}$ mice and paralleled increases seen for NCC. Losartan, HET0016, and 20-HETE antagonists each normalized SGK1 mRNA expression. These results point to a potential 20-HETE dependence of intrarenal angiotensinogen production and ANGII receptor type 1 activation that are associated with increases in NCC and SGK1 and identify elevated P450 4A11 activity and 20-HETE as potential risk factors for salt-sensitive human hypertension by perturbation of the renal renin-angiotensin axis.

Cytochrome P450 (CYP)[2] 4A11 is a major contributor to the formation of 20-hydroxyeicosatetraenoic acid (20-HETE) from arachidonic acid in human kidney (1–3). 20-HETE is a potent vasoconstrictor that is thought to contribute to the pressor actions of angiotensin II (ANGII), vasopressin, and endothelin, and has also been shown to increase natriuresis with a potential to lower blood pressure (BP) (4–6). The P450 4A11 variant F434S (rs1126742) reduces the catalytic efficiency (k_{cat}/K_m) of recombinant CYP4A11-catalyzed NADPH- and oxygen-dependent conversion of arachidonic acid to 20-HETE by roughly one-third (7). Similarly, another single nucleotide polymorphism, rs9332978 (in the promoter region of the *CYP4A11* gene), reduces reporter gene expression by about 30% (8). Genetic association studies suggest that the two SNPs and another, rs3890011 (which is in linkage disequilibrium with rs1126742), are associated with increased risk for hypertension and cardiovascular disease (7–16). CYP4A11 is expressed in the proximal tubule, the thick ascending limb, distal tubule, and collecting ducts, but CYP4A11 has not been detected in either glomeruli or renal vasculature or microvasculature (17). Consistent with this tissue distribution, the rs3890011 and rs1126742 mutations have been associated with disturbances of sodium and water homeostasis in humans that are likely to reflect changes in kidney function (12, 18, 19).

Earlier studies in our laboratory developed and characterized two human *CYP4A11* transgenic mouse lines, designated line B and line F, to examine the regulation of the human *CYP4A11* gene in an integrated physiologic model (20). These lines were generated by incorporation of the complete *CYP4A11* gene, including >45 kb of the upstream and >10 kb of downstream

* This work was supported by United States Public Health Service Grants R01 HD004445 (to E. F. J.) and P01 DK038226 (to J. H. C., J. R. F., and F. P. G.) and The Welch Foundation Grant I-0011 (to J. R. F.). The authors declare that they have no conflicts of interest with the contents of this article. The content of this manuscript is solely the responsibility of the authors and does not necessarily represent the official views of the National Institutes of Health.

[1] To whom correspondence should be addressed: MEM-255, 10550 North Torrey Pines Rd., La Jolla, CA 92037. E-mail: johnson@scripps.edu.

[2] The abbreviations used are: CYP, cytochrome P450; 20-HETE, 20-hydroxyeicosatetraenoic acid; BP, blood pressure; NCC, sodium chloride cotransporter; SGK1, serum glucocorticoid kinase 1; ANGII, angiotensin II; AGT, angiotensinogen; ATR1, ANGII receptor 1; B-129/Sv-4A11$^{+/+}$, homozygous line B carrying four *CYP4A11* gene copies; B-129/Sv-4A11$^{+/-}$, heterozygous line B carrying two *CYP4A11* gene copies; F-129/Sv-4A11$^{+/-}$, heterozygous line F carrying one *CYP4A11* gene copy; HET0016, *N*-hydroxy-*N*′-(4-*n*-butyl-2-methylphenyl)formamidine; 20-6,15-HEDGE, sodium 2-((6*Z*,15*Z*)-20-hydroxyicosa-6,15-dienamido)acetate; AAA, sodium (*S*)-2-((6*Z*,15*Z*)-20-hydroxyicosa-6,15-dienamido)succinate; HCTZ, hydrochlorothiazide; 11β-HSD2, 11β-hydroxysteroid dehydrogenase type 2; qPCR, quantitative PCR; UPLC, ultra-high performance liquid chromatography-tandem mass spectrometry.

flanking inter-gene regions, from human BAC clone RP11-345m5 to ensure that native *cis*-acting regulatory elements of the human gene are retained and potential effects of the insertion site on expression of the transgene are reduced. Among many tissues examined, the liver and kidney were found to be the predominant sites of *CYP4A11* transgene expression, which is consistent with tissue selectivity seen in humans. The CYP4A11 transgene expression level in mice was within the range of values seen for CYP4A11 expression in human liver and kidney (20, 21).

Augmented production of 20-HETE in several transgenic or genetically modified mouse models has been shown to elevate BP (4, 22–27). As expression of the human *CYP4A11* transgene in mice is likely to augment endogenous capacity to form 20-HETE in renal tubular epithelium, we determined the effect of the *CYP4A11* transgene on BP. Here, we present data to support CYP4A11-dependent augmentation of 20-HETE production as well as gene dosage-dependent development of salt-sensitive hypertension. Elevated BP is associated with an increase of angiotensinogen, NCC, and SGK1 expression in kidney, whereas plasma ANGII, aldosterone, and renin activity were unchanged. The use of inhibitors of CYP ω-hydroxylases, ANGII receptor 1 (ATR1), or NCC and 20-HETE antagonists demonstrate the reversibility of these processes and implicate these renal pathways in the development of the salt-sensitive hypertensive phenotype seen in *CYP4A11* transgenic mice.

Results

Increased Systemic BP in B-129/Sv-4A11$^{+/+}$ Mice and Normalization of BP by the P450 4A Inhibitor HET0016—B-129/Sv-4A11$^{+/+}$ mice are carriers of two haploid transgene copies and, as a result, this homozygous line has four copies of the *CYP4A11* gene (Fig. 1*A*). In contrast, hemizygous transgenic line B and line F congenic 129/Sv mice carry two copies and one copy of the transgene, respectively. Amplification of the murine *Cyp4a14* gene indicated that all three lines carried two copies of the endogenous gene, as expected. Statistically significant increases in BP were seen in the B-129/Sv-4A11$^{+/+}$ mice, as indicated by systolic BP values of 143 ± 8 mm Hg for B-129/Sv-4A11$^{+/+}$ females and 140 ± 7 mmHg for B-129/Sv-4A11$^{+/+}$ males compared with 110 ± 6 in female and 115 ± 10 in male wild-type mice (Fig. 1*B*). Although diastolic BP was also elevated in B-129/Sv-4A11$^{+/+}$ mice, systolic BP values are reported throughout the article. BP did not differ significantly between sexes within each genotype. Interestingly, congenic male and female hemizygote line B 129/Sv mice carrying two *CYP4A11* gene copies on one haploid chromosome (B$^{-/+}$) displayed normal BP of 111 ± 6 mm Hg (n = 13), and the independent congenic hemizygous *CYP4A11* transgenic line F 129/Sv male mice that carry only one copy of the *CYP4A11* gene (F$^{-/+}$) also exhibited normal BP (107 ± 11 mm Hg, n = 8). Treatment of hypertensive B-129/Sv-4A11$^{+/+}$ mice with HET0016, a selective inhibitor of fatty acid ω-hydroxylases (including CYP4A11 (28, 29)) normalized BP, and after administration of HET0016 was discontinued, BP returned to the elevated levels observed before treatment (Fig. 1*C*). Collectively, these results show that the presence of four copies of the *CYP4A11* gene in the 129/Sv background increases systemic BP in mice; in addition, the hypertensive phenotype is reversible and is likely to reflect the catalytic activity of P450 4A11 because HET0016 normalized BP in the transgenics without signifi-

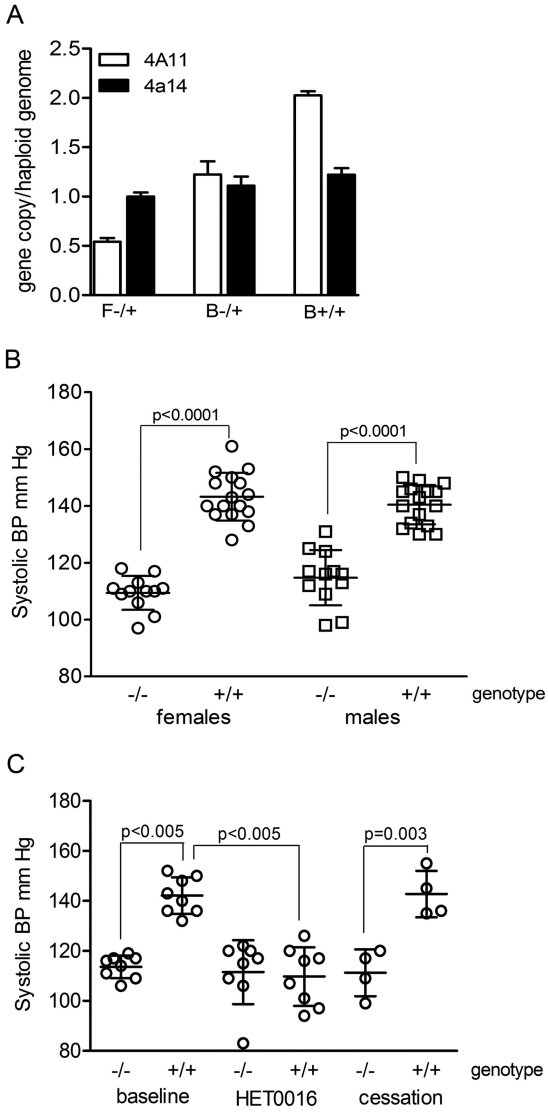

FIGURE 1. *A*, *CYP4A11* transgene copy numbers. Transgene copy numbers were determined using genomic DNA isolated from tail clippings of CYP4A11 transgenic lines F-129/Sv-4A11$^{-/+}$ (F−/+), B-129/Sv-4A11$^{-/+}$ (B−/+), and B-129/Sv-4A11$^{+/+}$ (B+/+) by qPCR as described under "Experimental Procedures." *Cyp4a14* gene copies were determined and are shown as an example of a haploid single-copy gene control. The mean ± S.D. is shown for biological replicates of each strain (F−/+, n = 6; B−/+, n = 6; B+/+, n = 12). *B*, systolic BP increases in B-129/Sv-4A11$^{+/+}$ mice. Non-invasive tail-cuff BP measurements were conducted in conscious females (*circles*) and males (*squares*) at 16–22 weeks of age as described under "Experimental Procedures." Each symbol represents an average systolic BP value for a single mouse that was determined from daily BP recordings of 20 measurements per session per day on at least five consecutive days. The mean ± S.D. for each group are indicated by the *long* and *short horizontal lines*, respectively, for biological replicates (−/− females, n = 12; +/+ females, n = 16; −/− males, n = 12; +/+ males, n = 16). Statistical significance for the effects of genotype *versus* sex was determined by two-way analysis of variance. A significant difference between females and males within genotypes was not seen (p = 0.6). *C*, BP is normalized by the P450 4A inhibitor HET0016 in B-129/Sv-4A11$^{+/+}$ mice. BP was recorded in female wild-type mice (−/−) and B-129/Sv-4A11$^{+/+}$ (+/+) mice at 16 weeks of age prior to treatment (baseline). HET0016 was then administered daily and BP recorded after 1 week (HET0016) as well as 3 weeks after the final treatment (cessation). Each *circle* represents the average systolic BP values for each mouse and mean ± S.D. are shown for each group (baseline, n = 8 per group; HET0016, n = 8 per group; cessation, n = 4 per group).

TABLE 1

Plasma and urine measurements

Plasma values represent the average of five biological replicates. For urine measurements, each urine sample was collected from two mice that were housed in a single metabolic cage and thus constitute one biological sample. The number of biological samples for urine values reported here is as follows: female 4A11$^{-/-}$ ($n = 8$); female 4A11$^{+/+}$ ($n = 8$); male 4A11$^{-/-}$ ($n = 3$); male 4A11$^{+/+}$ ($n = 4$). Urinary excretion of electrolytes per mouse represents the measured urinary concentration of the indicated component multiplied by urine volume and divided by the number of mice in the metabolic cage. Values are expressed as the mean ± S.D.

	4A11$^{-/-}$	4A11$^{+/+}$	Tg/Wt ratio	*p* value
	Mean ± S.D.			
Females				
Body weight, g	18.1 ± 0.7	18.93 ± 1.6	1.05	0.19
Plasma BUN, mg/dl	25.6 ± 2.7	27.6 ± 6.9	1.08	0.56
Plasma creatinine, mg/dl	0.2 ± 0.0	0.2 ± 0.0	1.00	0.17
Plasma sodium, mM	152 ± 4	148 ± 2	0.98	0.10
Plasma potassium, mM	6.7 ± 0.6	7.9 ± 0.6	1.18	0.01[a]
Urinary excretion				
Urine, ml/mouse/day	0.82 ± 0.15	0.51 ± 0.08	0.63	<0.01[a]
Creatinine, mg/day	0.27 ± 0.05	0.21 ± 0.06	0.78	0.05
Sodium, mEq/day	0.16 ± 0.02	0.15 ± 0.04	0.92	0.40
Potassium, mEq/day	0.24 ± 0.04	0.18 ± 0.05	0.75	0.01[a]
Chloride, mEq/day	0.26 ± 0.03	0.21 ± 0.05	0.79	0.02[a]
Calcium, mg/day	0.15 ± 0.04	0.08 ± 0.04	0.55	<0.01[a]
Males				
Body weight, g	23.7 ± 2.8	24.8 ± 0.6	1.05	0.45
Plasma BUN, mg/dl	23.2 ± 2.7	27.4 ± 1.7	1.11	0.10
Plasma creatinine, mg/dl	0.2 ± 0.0	0.2 ± 0.0	1.00	0.50
Plasma sodium, mM	157 ± 13	158 ± 11	1.00	0.94
Plasma potassium, mM	6.36 ± 0.73	7.46 ± 0.43	1.17	0.02[a]
Urinary excretion				
Urine, ml/mouse/day	0.60 ± 0.05	0.44 ± 0.03	0.73	<0.01[a]
Creatinine, mg/day	0.29 ± 0.03	0.23 ± 0.07	0.79	0.20
Sodium, mEq/day	0.15 ± 0.02	0.10 ± 0.01	0.66	<0.01[a]
Potassium, mEq/day	0.24 ± 0.01	0.15 ± 0.02	0.63	<0.01[a]
Chloride, mEq/day	0.25 ± 0.02	0.15 ± 0.02	0.59	<0.01[a]
Calcium, mg/day	0.10 ± 0.02	0.07 ± 0.01	0.72	0.02[a]

[a] Statistically significant differences between genotypes are *p* values <0.05.

TABLE 2

ANGII, aldosterone, and renin concentrations in blood

Blood was collected from male mice at weeks 18–19 of age. ANGII and renin levels were determined in plasma and aldosterone was measured in serum. Blood samples for ANGII and aldosterone were collected on two different days and thus represent two independent collections. Samples for renin measurements were obtained on a single day. The values represent means ± S.D. with the number of mice shown in parentheses.

	4A11$^{-/-}$	4A11$^{+/+}$	*p* value
ANGII pg/ml (plasma)	62.5 ± 49.9 ($n = 7$)	59.2 ± 23.4 ($n = 7$)	0.64
Aldosterone pg/ml (serum)	162 ± 95 ($n = 6$)	152 ± 79 ($n = 7$)	0.84
Renin activity ng/ml/h (plasma)	201 ± 49 ($n = 3$)	171 ± 65 ($n = 3$)	0.23

cantly affecting the wild-type mice. As the hypertensive phenotype was only seen in B-129/Sv-4A11$^{+/+}$ mice, all subsequently reported results here were conducted in this line and wild-type 129/Sv control mice.

Urine and Blood Chemistry Differences in B-129/Sv-4A11$^{+/+}$ Compared with Wild-type Mice—B-129/Sv-4A11$^{+/+}$ male and female mice exhibited 25 and 30% reduction of urine output, respectively, relative to wild-type mice ($p < 0.0005$ for females and males with *n* of at least 17 per group). The daily excretion of several electrolytes including potassium and chloride was lower in both sexes, whereas decreased sodium excretion was only statistically significant in male transgenic mice (Table 1). Interestingly, urinary calcium levels were also decreased, but total protein excretion was not affected (data not shown). Analysis of blood samples indicated that with the exception of potassium, which was elevated by about 18%, plasma concentrations of other electrolytes were normal. Plasma creatinine and blood urea nitrogen values were in the normal range as were levels of biomarkers for tissue damage. The differences in electrolyte excretion suggested that circulating components of the renin-angiotensin-aldosterone system might be affected. Nevertheless, measurements of plasma renin activity, ANGII, and aldosterone concentrations showed no significant differences between B-129/Sv-4A11$^{+/+}$ and control mice (Table 2).

A Low Salt Diet Normalizes BP and Eliminates Differences in Urine and Electrolyte Output between Transgenic and Wild-type Mice—To test the salt dependence of the hypertension exhibited by B-129/Sv-4A11$^{+/+}$, we placed transgenic and control mice on a low salt diet containing 0.1% sodium chloride. The BP of B-129/Sv-4A11$^{+/+}$ was reduced to normal levels after 21 days on the low salt diet, whereas that of wild-type mice did not change significantly (Fig. 2). The responses were similar in males and females. Under these conditions, no significant differences in urine volumes, creatinine, and electrolyte excretion were evident between transgenic and wild-type strains (Table 3). The association of salt-sensitive hypertension with low plasma renin activity, low plasma aldosterone concentrations, low urine output, and elevated plasma potassium is similar to the phenotype exhibited by genetically engineered mice that express a mutant form of the With No Lysine Kinase (WNK4) protein (30). This mutation of WNK4 is associated with a familial human disorder pseudo-hyperaldosteronism type 2 that leads to increased accumulation of the thiazide-sensitive NCC, which increases sodium uptake in the distal convoluted tubule.

Evidence for Activation of NCC in B-129/Sv-4A11$^{+/+}$ Mice—To test whether hypertension in B-129/Sv-4A11$^{+/+}$ mice on a normal salt diet is related to increased NCC activity, we treated mice with the NCC inhibitor hydrochlorothiazide (HCTZ). HCTZ normalized BP in B-129/Sv-4A11$^{+/+}$ mice but did not affect BP in wild-type mice (Fig. 3*A*), suggesting that increased NCC activity contributes to the observed hypertension. In contrast, treatment of mice with amiloride, which targets the epithelial sodium channel (ENaC), did not alter BP in B-129/Sv-4A11$^{+/+}$ or wild-type mice (Fig. 3*B*). Estimation of NCC protein levels by immunoblotting revealed an ~1.5-fold elevation of protein in B-129/Sv-4A11$^{+/+}$ kidneys relative to controls (Fig. 4). Phosphorylation of the amino-terminal domain of NCC has been suggested as a mechanism of NCC activation, and elimination of phosphorylation sites Ser-71, Thr-58, and Thr-53 prevented a response of NCC to intracellular chloride depletion (31). Additional studies reported that phosphorylation at the Thr-58 residue is absolutely necessary for NCC activity, whereas Thr-53 and Ser-71 phosphorylation are additionally required for its full activity (32). To compare NCC phosphorylation status in wild-type and transgenic mice, antibodies were used that specifically recognize phosphorylation at residues Thr-53, Thr-58, Ser-71, or Ser-89, respectively (33). Immunoblotting showed that phosphorylation of NCC was increased at all four residues in kidneys from B-129/Sv-4A11$^{+/+}$ mice compared with wild-type (Fig. 4). As the ratio of pNCC to NCC remains constant (Fig. 4*C*), phosphorylated NCC increases in parallel with the abundance of total NCC

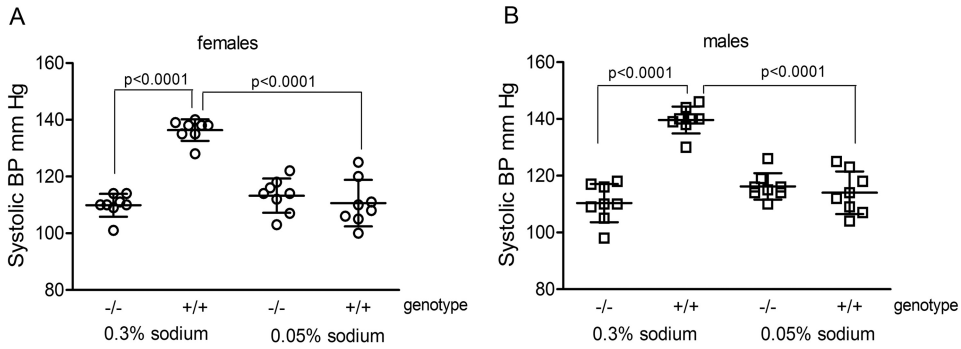

FIGURE 2. **Salt sensitivity of BP in B-129/Sv-4A11$^{+/+}$ mice.** Baseline BP was measured in females (*A*) and males (*B*) that were given a normal salt diet (0.3% sodium). Mice were then switched to a low-salt diet (0.05% sodium) for 3 weeks, and BP was recorded daily on days 14 to 21. Each *circle* or *square* represents an average systolic BP value collected for a single mouse at 20 BP recordings per session per day over a period of 5 days. The mean ± S.D. are presented for each group with 8 biological replicates per group. Statistical significance was determined by pairwise comparison and is depicted by the *p* values.

TABLE 3

Urine chemistry on low salt diet

Mice were given a low salt diet for three weeks and transferred to metabolic cages (four mice per cage) for overnight urine collections while maintained on a low salt diet. Each value represents a measurement obtained from one urine pool obtained from four mice.

	Experiment 1		Experiment 2	
	4A11$^{-/-}$	4A11$^{+/+}$	4A11$^{-/-}$	4A11$^{+/+}$
Females				
Urine, ml/mouse/day	0.48	0.55	0.40	0.43
Creatinine, mg/day	0.19	0.27	0.16	0.19
Sodium, mEq/day	0.02	0.02	0.01	0.02
Potassium, mEq/day	0.14	0.18	0.15	0.16
Chloride, mEq/day	0.07	0.08	0.06	0.07
Calcium, mg/day	0.07	0.14	0.05	0.02
Males				
Urine, ml/mouse/day	0.55	0.53	0.60	0.63
Creatinine, mg/day	0.20	0.21	0.16	0.21
Sodium, mEq/day	0.05	0.04	0.02	0.02
Potassium, mEq/day	0.15	0.16	0.15	0.18
Chloride, mEq/day	0.07	0.07	0.08	0.07
Calcium, mg/day	0.09	0.08	0.02	0.07

protein in B-129/Sv-4A11$^{+/+}$ mice. Furthermore, the use of P450 4A inhibitor HET0016 attenuated the increase of total and phosphorylated NCC in B-129/Sv-4A11$^{+/+}$ mice without affecting wild-type mice (Fig. 5), suggesting an association of P450 4A activity with the increase in abundance of normally phosphorylated NCC protein. This increase does not appear to reflect elevated transcription because NCC mRNA levels remained unchanged in B-129/Sv-4A11$^{+/+}$ compared with wild-type ($p = 0.68$, $n = 10$). The accumulation of NCC protein in transgenic animals could potentially be a consequence of decelerated turnover, which is similar to the effects of constitutively active WNK4 variants, which reduce NCC turnover by suppressing its ubiquitination (30).

The Renal Renin-Angiotensin System Is Activated in B-129/Sv-4A11$^{+/+}$ Mice—The reduction in urine volume and electrolyte elimination combined with increases in BP suggested that the renin-angiotensin system might be more active in B-129/Sv-4A11$^{+/+}$ mice. ANGII stimulates NCC activity (34) and can do so independently of aldosterone (35). Although plasma renin activity and ANGII concentrations are not altered in these transgenic mice, the distal nephron could see an increased ANGII exposure due to locally increased synthesis of ANGII in the kidney. ANGII is produced by cleavage of the 10 N-terminal amino acids from angiotensinogen (AGT) by renin to generate ANGI, which is cleaved by angiotensin converting enzyme 1 (ACE-1) to produce the octapeptide ANGII. The actions of ANGII are mediated by ATR1 and serve to regulate BP, electrolyte, and water balance. As the kidney expresses all of the components necessary for generation of ANGII (36), quantitative PCR (qPCR) was employed to compare steady-state mRNA levels of components of the renin-angiotensin system in kidneys of B-129/Sv-4A11$^{+/+}$ and wild-type mice. Nearly 2-fold increases of AGT mRNA were noted in B-129/Sv-4A11$^{+/+}$ mice (Fig. 6), whereas specific mRNAs for ATR1, renin-1, and renin-2 were largely unchanged in B-129/Sv-4A11$^{+/+}$ mice. Increases seen for ACE1 mRNA were 1.2-fold higher in the transgenic animals and statistically significant only in females, whereas ACE2 mRNA levels were unaffected (Fig. 6). Additionally, we assessed whether expression of mRNAs encoding the 11β-hydroxysteroid dehydrogenase, type 2 (11β-HSD2), were affected by the transgene, as a reduction in 11β-HSD2 expression could lead to activation of the mineralocorticoid receptor by normal circulating concentrations of corticosterone and stimulate an increase of NCC abundance (37). As shown in Fig. 6, renal levels of 11β-HSD2 mRNA were not affected by the *CYP4A11* transgene.

Next we addressed the question of whether increased AGT expression can be affected by inhibition of P450 4A activity. Indeed, AGT mRNA increases seen in transgenic mice were decreased after treatment with HET0016 (Fig. 7*A*), suggesting that the elevation of AGT expression reflects the catalytic activity of the *CYP4A11* transgene product and that reduction of AGT expression is associated with normalization of BP by HET0016. The observed increases of AGT mRNA led to the hypothesis that intrarenal ANGII may be increased proportionally and, in turn, increase signaling via ATR1. Consistent with this notion, blockade of ATR1 by losartan normalized BP when administered to female B-129/Sv-4A11$^{+/+}$ mice, but losartan did not significantly affect BP in female control mice (Fig. 7*B*). The normalization of BP by losartan was paralleled by normalization of increased renal AGT mRNA seen in transgenic mice (Fig. 7*C*). Comparison of renal AGT mRNA levels under conditions of normal and low salt diets revealed that the increases of AGT mRNA in transgenic mice on a normal salt diet is similar to that observed when AGT mRNA expression are stimulated by systemic activation of the renin angiotensin aldosterone sys-

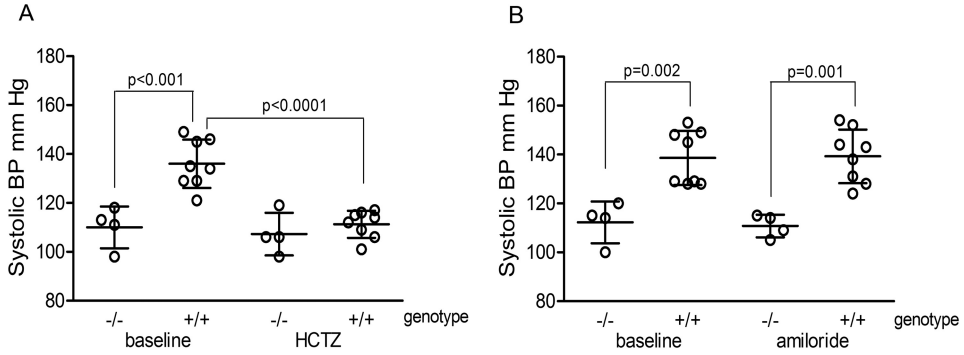

FIGURE 3. **The NCC inhibitor HCTZ normalizes BP in B-129/Sv-4A11$^{+/+}$, but the ENAC inhibitor amiloride does not.** Baseline BP was determined in female wild-type (−/−) and B-129/Sv-4A11$^{+/+}$ (+/+) mice prior to HCTZ (*A*) or amiloride (*B*) administration and BP recorded daily on days 5–8 of treatment with each compound. Each *symbol* represents average systolic BP values for each mouse with ± S.D. reflecting the variation within each experimental group (−/−, n = 4; +/+, n = 8). Statistical significance was determined by pairwise comparison and is depicted by the p values.

tem in wild-type animals on a sodium-restricted diet, irrespective of genotype (Fig. 7*D*).

CYP4A11 Transgene Expression in Mice Augments in Vivo 20-HETE Production—To determine the impact of *CYP4A11* transgene expression on steady-state levels of 20-HETE *in vivo*, 20-HETE was quantified in urine and lipid extracts from kidney homogenates. Measurements of urinary 20-HETE indicated a 2-fold elevation of this metabolite in male B-129/Sv-4A11$^{+/+}$ mice and a 3-fold increase in female B-129/Sv-4A11$^{+/+}$ mice compared with the corresponding wild-type mice (Fig. 8*A*). In addition to treatment with β-glucuronidase, tissue extracts were subjected to mild alkaline hydrolysis to free 20-HETE esterified to glycerolipids. Mean concentrations of 20-HETE in kidney homogenates from male (21.6 ng/g tissue) and female (20.4 ng/g) B-129/Sv-4A11$^{+/+}$ mice were 1.7- and 3.3-fold higher, respectively, than of male (12.7 ng/g) and female (6.1 ng/g) wild-type mice (Fig. 8*B*). However, plasma 20-HETE levels did not differ between wild-type and B-129/Sv-4A11$^{+/+}$ mice (data not shown). Furthermore, treatment with losartan decreased 20-HETE production in the kidneys of B-129/Sv-4A11$^{+/+}$ mice, as measured in extracts (Fig. 8*C*). Collectively, these results indicate that the steady-state amounts of 20-HETE were increased in kidneys of B-129/Sv-4A11$^{+/+}$ mice and that these levels were reduced by ATR1 blockade. Although changes in arachidonic acid availability (as well as reduced degradation by alternative metabolic pathways such as mitochondrial or peroxisomal β-oxidation) could contribute to this increase, these results suggest that expression of the transgene augmented the capacity for 20-HETE formation. Moreover, this is likely to reflect the presence of the P450 4A11 enzyme because mRNA expression of major murine *Cyp4a* genes indicated that *Cyp4a12a*, *Cyp4a10*, and *Cyp4a14* gene expression is not altered by the presence of the *CYP4A11* transgene (Fig. 9). Cyp4a12b mRNA is increased about 2-fold in transgenics; however, the relative abundance of Cyp4a12b compared with Cyp4a12a is 2 orders of magnitude lower, and the impact of this change is likely to be small.

To test if the effects of the *CYP4A11* transgene reflect the increased synthesis of 20-HETE, female B-129/Sv-4A11$^{+/+}$ and control mice were treated with sodium 2-((6*Z*,15*Z*)-20-hydroxyicosa-6,15-dienamido)acetate (20-6,15-HEDGE). This compound is a more soluble and metabolically stable analog of 20-HEDE (20-hydroxyeicosa-6(*Z*),15(*Z*)-dienoic acid) that antagonizes the vasoconstrictive effects of 20-HETE in *ex vivo* experiments (38) and normalizes BP in genetically modified hypertensive mice that produce elevated 20-HETE (27). 20-6,15-HEDGE normalized BP in B-129/Sv-4A11$^{+/+}$ mice without significantly affecting BP in control mice (Fig. 10*A*). This result was corroborated using a second, more soluble analog, sodium (*S*)-2-((6*Z*,15*Z*)-20-hydroxyicosa-6,15-dienamido)-succinate (AAA), which also normalized BP in male B-129/Sv-4A11$^{+/+}$ mice without significant effects on BP of control mice (Fig. 10*B*). The two compounds are the glycine and aspartic acid amide conjugates of the 20-HETE antagonist 20-HEDE, the lead compound that was first shown to potently antagonize the vasoconstrictive effects of 20-HETE (38). Treatment with either one of these compounds alleviated the increase of AGT mRNA seen in B-129/Sv-4A11$^{+/+}$ mice (Fig. 10, *C* and *D*) and paralleled the effects of HET0016, even though 20-6,15-HEDGE does not affect 20-HETE formation (39).

SGK1 Expression is Elevated in B-129/Sv-4A11$^{+/+}$ Mice and the Increases Are Reversed by Antagonism of 20-HETE—SGK1 contributes to the regulation of ion transporter activity (40). Stimulation of *SGK1* gene transcription by aldosterone activation of the mineralocorticoid receptor contributes to enhanced uptake of sodium ions by NCC and ENAC in the mineralocorticoid responsive portion of the nephron by inhibition of protein turnover, but the role of SGK1 in the effects of ANGII on NCC activity has not been established. However, ANGII has been reported to induce SGK1 expression in cultured human and mouse fibroblasts (41, 42) and in primary cultures of human proximal tubule cells (43). Moreover, the ATR1 antagonist losartan lowers plasma and renal ANGII levels and renal SGK1 expression in spontaneously hypertensive rats (44). Based on these observations, we examined whether renal SGK1 mRNA and protein expression are elevated in B-129/Sv-4A11$^{+/+}$ mice relative to wild-type controls. A 2–3-fold increase in both SGK1 protein and mRNA was evident in B-129/Sv-4A11$^{+/+}$ mice (Fig. 11, *A*–*C*). The increases of SGK1 protein were paralleled by similar increases of NCC protein (Fig. 11, *A* and *B*) and elevated SGK1 and NCC proteins were restored to control levels by treatment with the 20-HETE antagonist AAA (Fig. 11, *A* and *B*). Increases seen for SGK1 mRNA in B-129/Sv-4A11$^{+/+}$ are alleviated in these mice in the

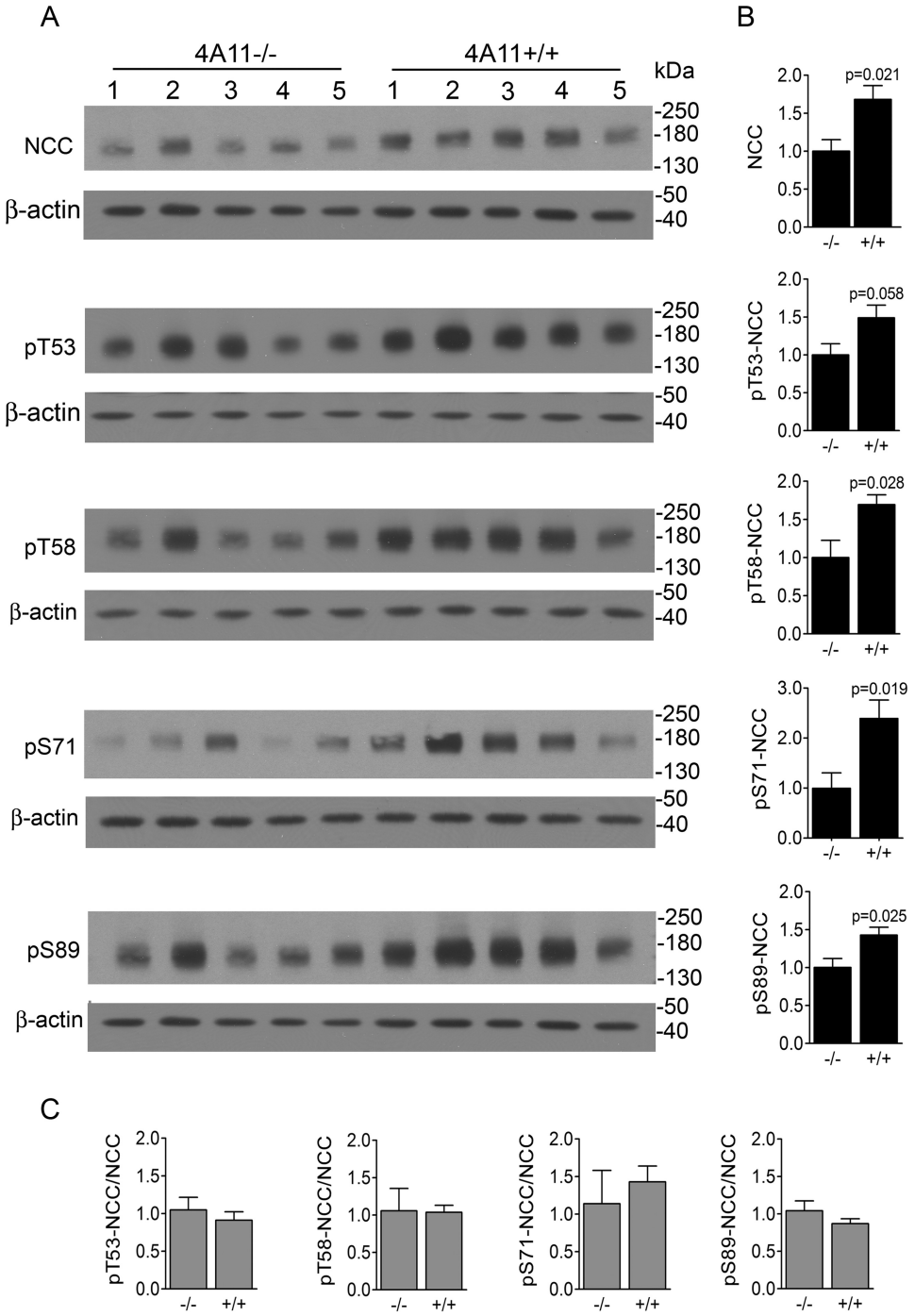

FIGURE 4. **Accumulation of NCC protein in B-129/Sv-4A11$^{+/+}$ is paralleled by increases of phosphorylated NCC.** *A*, 100,000 × *g* protein pellets were prepared from wild-type (4A11−/−) and B-129/Sv-4A11$^{+/+}$ (4A11+/+) mouse kidneys and subjected to immunoblotting using anti-NCC or antibodies that recognize NCC phosphorylation at residue Thr-53, Thr-58, Ser-71, or Ser-89, respectively. *Lanes 1–5* represent biological replicates for each group. *B*, quantitation of NCC protein. Values represent means of normalized target/β-actin ratios ± S.E. for five biological replicates per group. Statistical significance is indicated by the *p* values. Similar increases of NCC protein (1.4-fold; $p = 0.008$, $n = 7$) were measured in two additional experiments in which 10,000 × *g* supernatants were immunoblotted (experiment 1 consisted of three biological replicates per 4A11$^{-/-}$ and 4A11$^{+/+}$ group, and experiment 2 consisted of four biological replicates per group). *C*, phosphorylated NCC/NCC ratios. Values represent mean ratios ± S.E. for five biological replicates per experimental group. Differences between wild-type (−/−) and B-129/Sv-4A11$^{+/+}$ (+/+) were examined by pairwise comparison and were found not be statistically significant ($p > 0.05$).

presence of the antagonist and even further reduced in wild-type control mice (Fig. 11*C*) as well as in the presence of the P450 4A inhibitor HET0016 (Fig. 11*D*) and by losartan (Fig. 11*E*). A comparison of the levels of SGK1 mRNA expression in mice on normal *versus* low salt diet showed that the elevation of SGK1 mRNA in B-129/Sv-4A11$^{+/+}$ mice on normal salt is similar to the level of SGK1 mRNA in control and transgenic mice on a low salt diet (Fig. 11*F*), indicating that the increase of SGK1 mRNA abundance in B-129/Sv-4A11$^{+/+}$ mice is likely to have a significant impact. The results of the 20-HETE antagonist on the regulation of SGK1 expression in B-129/Sv-4A11$^{+/+}$ mice could reflect a direct effect of 20-HETE on transcriptional reg-

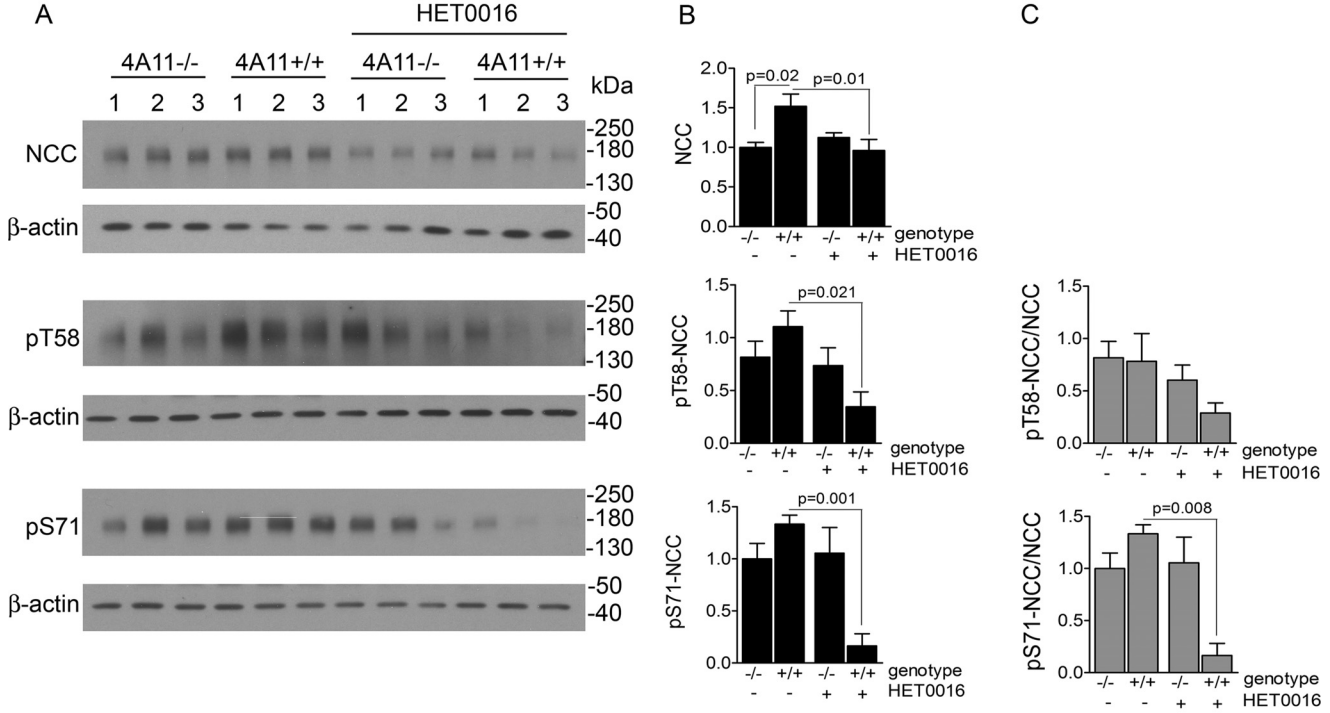

FIGURE 5. **The P450 4A inhibitor HET0016 reverses the increases of NCC protein and attenuates its phosphorylation status.** *A*, upon completion of HET0016 treatment and verification of BP normalization, kidney homogenates from 10,000 × *g* supernatants were immunoblotted using anti-NCC or antibodies that recognize NCC that is phosphorylated at the Thr-58 and Ser-71 residue, respectively. Numbers *1–3* represent biological replicates per experimental group. *B*, quantitation of immunoblots. NCC or pNCC signals were normalized to signals obtained for β-actin and normalized values were presented as mean ± S.E. Biological replicates for NCC bar graph: −/− without HET0016, $n = 6$; +/+ without HET0016, $n = 7$; −/− with HET0016, $n = 6$; +/+ with HET0016 $n = 7$; pT58 and pS71 graphs: three biological replicates per experimental group. Statistical significance is indicated by the *p* values. *C*, phosphorylated NCC/NCC ratios. Values represent mean ratios ± S.E. for 3 biological replicates per group. A statistically significant change is depicted by the *p* value.

ulation of *SGK1* or an indirect effect as a consequence of suppression of AGT expression in the proximal tubule.

To further examine the association of changes in SGK1, AGT, and NCC expression with the hypertensive phenotype, we characterized whether SGK1, AGT, and NCC expression is affected in hemizygous line B transgenics, which exhibit normal BP. As expected, CYP4A11 mRNA expression was increased in homozygous B-129/Sv-4A11$^{+/+}$ over hemizygous B-129/Sv-4A11$^{+/-}$ mice that have only one copy of the *CYP4A11* tandem repeat (Fig 12*A*). AGT mRNA was only increased by about 30% in B-129/Sv-4A11$^{+/-}$ compared with wild-type controls ($p = 0.06$); however, AGT mRNA abundance was significantly elevated in the homozygous transgenics relative to the hemizygous line B mice (Fig 12*B*). SGK1 mRNA was unchanged in hemizygous line B relative to wild-type mice, but increased 2-fold in homozygous line B transgenic mice (Fig. 12*C*). SGK1 and NCC protein levels did not differ significantly between wild-type and line B hemizygous mice (Fig. 12, *D* and *E*). These results strengthen the association of the hypertensive phenotype with increased abundance of AGT, SGK1, and NCC in B-129/Sv-4A11$^{+/+}$ mice.

Discussion

This study addressed whether expression of the human *CYP4A11* gene with its native promoter in mice alters their BP and whether changes in BP are related to a change in 20-HETE production. Our results showed that although carriers of one or two *CYP4A11* gene copies exhibited normal BP, 129/Sv mice carrying four *CYP4A11* gene copies developed hypertension on a normal salt diet regardless of gender. The hypertensive phenotype of B-129/Sv 4A11$^{+/+}$ mice resembles Gordon syndrome (45), or pseudohyperaldosteronism type 2, because blood potassium ion concentrations were increased by 18%, plasma concentrations of aldosterone and ANGII as well as plasma renin activity did not differ from wild-type controls, and dietary restriction of sodium intake normalized BP to levels seen in wild-type mice. Hypertensive B-129/Sv-4A11$^{+/+}$ mice also exhibited reduced urinary excretion of electrolytes and urine output. As seen in Gordon syndrome, transgenic mice show elevated steady-state levels of NCC protein, and the hypertension is normalized by treatment with the NCC inhibitor HCTZ. In contrast, amiloride, an inhibitor of the epithelial sodium channel, did not reduce the hypertension seen in the B-129/Sv-4A11$^{+/+}$ mice. Importantly, the P450 4A inhibitor HET0016 normalized BP and decreased NCC in B-129/Sv-4A11$^{+/+}$ mice to control levels thus linking the elevation of BP to the activity of the *CYP4A11* transgene product. Additionally, 20-HETE antagonists normalized blood pressure and NCC abundance suggesting that the phenotype was related to the increased formation of 20-HETE in the transgenic mice. The elevation of NCC abundance and the normalization of salt-sensitive hypertension by the NCC inhibitor HCTZ was surprising because 20-HETE reduces sodium uptake in kidney epithelial cells in experimental models that induce hypertension (5, 6). Moreover, hypertension is not salt-sensitive in two other

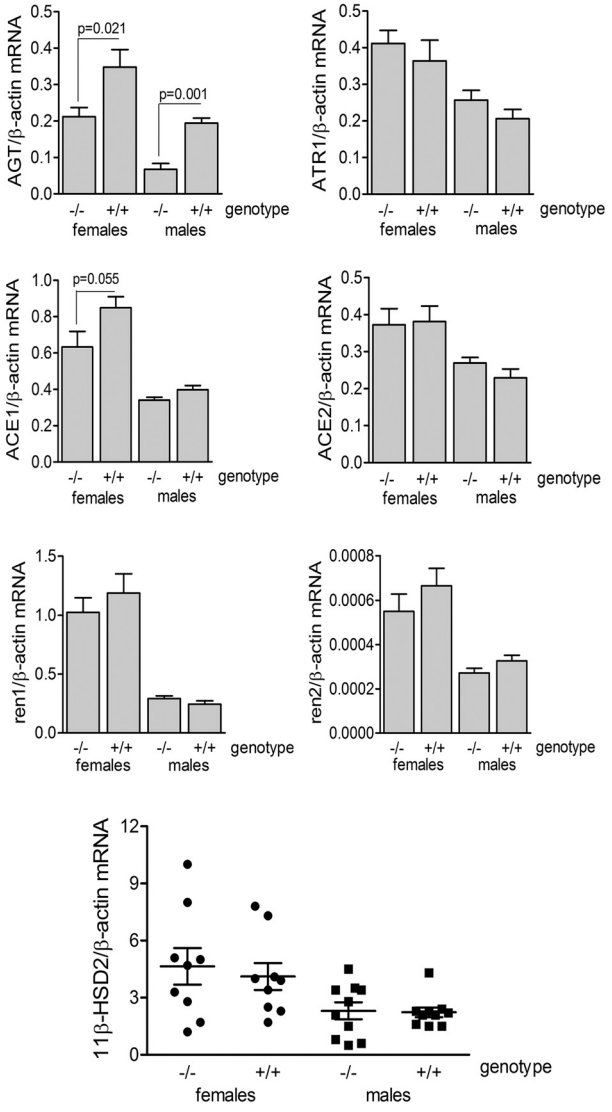

FIGURE 6. **Quantitative PCR of mRNA for components of the kidney renin-angiotensin system and 11β-*HSD2*.** B-129/Sv-4A11$^{+/+}$ kidney RNA was reverse transcribed and subjected to qPCR using specific primers for angiotensinogen (*AGT*), angiotensin 2 receptor 1 (*ATR1*), angiotensin converting enzyme 1 and 2 (*ACE1* and *ACE2*), renin-1 and renin-2 (*ren1* and *ren2*), 11β-HSD2, and β-actin. The CYP4A11 genotype is indicated by (−/−) and (+/+). Values represent average target/β-actin mRNA ratios ± S.E. depicting the variation within each group for 10 biological replicates for the components of the renin-angiotensin system. Biological replicates for 11β-HSD2/β-actin mRNA are as follows: −/− females, $n = 9$; +/+ females, $n = 9$; −/− males, $n = 10$; +/+ males, $n = 10$. Statistically significant changes in the steady-state mRNA level for the −/− *versus* +/+ genotype within each sex are depicted by *p* values.

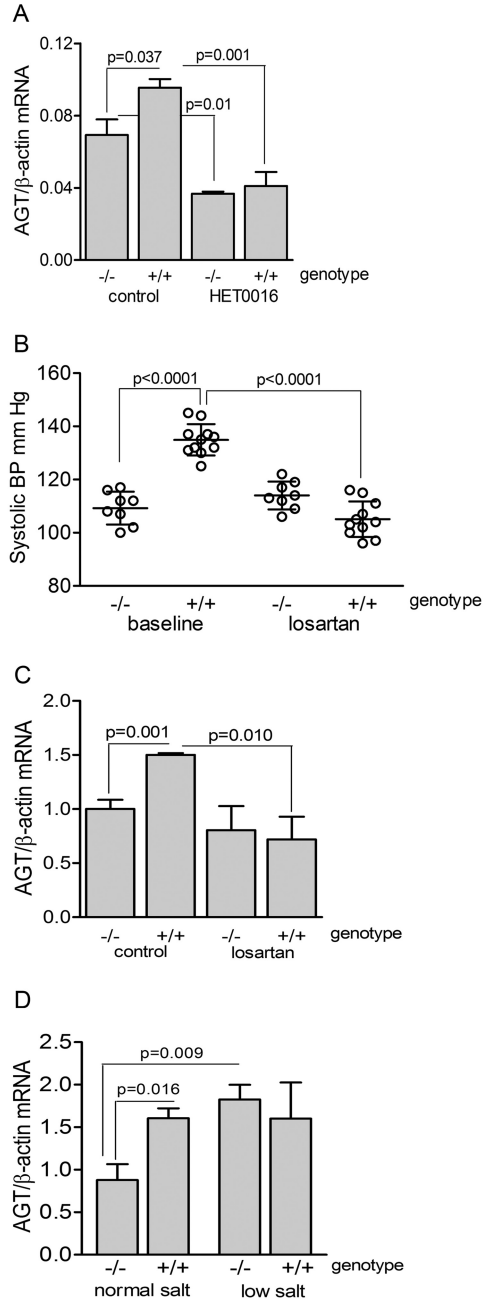

FIGURE 7. *A*, increases of renal AGT mRNA in B-129/Sv-4A11$^{+/+}$ are diminished by administration of HET0016. Steady-state mRNA of AGT and β-actin mRNA levels in kidneys of female mice in the absence of HET0016 (control) and after treatment with HET0016. Values represent means ratios ± S.E. of AGT/β-actin with an $n = 4$ per experimental group. *B*, BP is normalized by the ATR1 blocker losartan in B-129/Sv-4A11$^{+/+}$ mice. Female mice were given losartan in their drinking water for 1 week, and BP was monitored on days 3 through 6. Each *symbol* represents average systolic BP values for each mouse with ± S.D. reflecting the variation within each experimental group ($n = 8$ for −/−; $n = 12$ for +/+). Statistically significant responses between groups are depicted by *p* values. *C*, AGT-specific mRNA increases are normalized by losartan. Values represent means ratios ± S.E. of AGT/β-actin mRNA for 4 biological replicates per group. *D*, AGT/β-actin mRNA determined from kidneys of mice that were given a normal salt or kept on a low salt diet for 3 weeks ($n = 4$). Statistically significant changes are depicted by the *p* values.

genetically modified mouse models with elevated formation of 20-HETE as a result of disruption of the *Cyp4a14* gene leading to elevated circulating androgens, which increase the expression of the endogenous *Cyp4a12a* (46) or in a mouse model where a human *CYP4F2* transgene is expressed in a number of tissues and cellular sites under control of an androgen-responsive promoter (47). These differences are likely to reflect differences in the nephron segments where 20-HETE is formed and/or differences in catalytic properties of CYP4A11, Cyp4a12a, and CYP4F2.

ANGII is known to increase NCC abundance independently of aldosterone via changes in the abundance of phosphorylated NCC and reduction of NCC ubiquination, which leads to increased NCC activity (48). Although systemic activation of the renin-angiotensin-aldosterone regulatory system was not evident in B-129/Sv-4A11$^{+/+}$ mice, localized activation of this

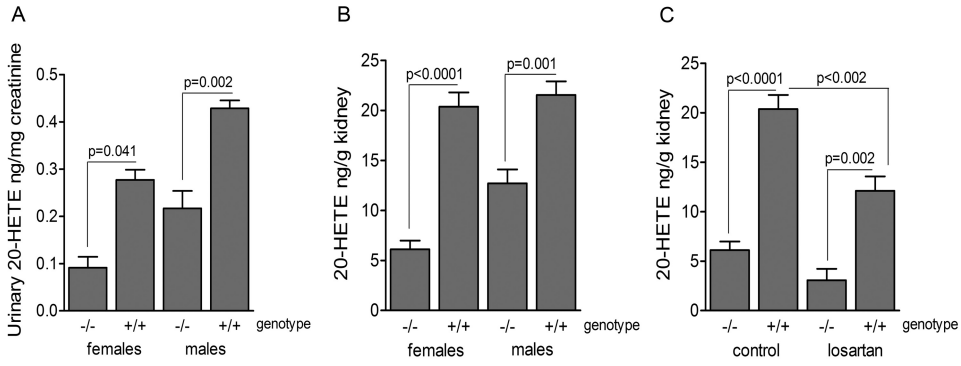

FIGURE 8. **Elevated urinary and kidney 20-HETE in B-129/Sv-4A11$^{+/+}$ mice.** *A*, mean urinary 20-HETE concentrations are expressed as ng/mg of creatinine ± S.E. Overnight urine collections were obtained as follows: −/− or +/+ females, average value was determined from three consecutive daily urine collections from 4 females that were housed in one cage (three technical replicates); −/− males, one overnight urine collection per cage, housing three, two, two, and three mice per cage (4 biological replicates); +/+ males, 4 cages of two mice per cage (four biological replicates). Significant differences are depicted by *p* values. *B*, whole kidney extracts from wild-type (−/−) or B-129/Sv-4A11$^{+/+}$ (+/+) mice were subjected to β-glucuronidase treatment, lipid extraction, and saponification. 20-HETE was determined in extracts by UPLC-MS/MS analysis. The values represent mean ± S.E. for biological replicates as follows: −/− females, $n = 10$; +/+ females, $n = 6$; −/− males, $n = 8$; +/+ males, $n = 6$. Statistically significant differences for −/− *versus* +/+ genotype within each sex are indicated by *p* values. *C*, treatment of female mice with losartan decreases 20-HETE production in B-129/Sv-4A11$^{+/+}$ mice. Mice were given losartan for 6 days. After determination that losartan decreased BP, mice were euthanized, and kidneys were subjected to whole tissue extraction as described. The values represent mean ± S.E. for biological replicates: −/− controls, $n = 10$; +/+ controls, $n = 6$; −/− losartan, $n = 4$; +/+ losartan, $n = 8$. Statistically significant responses are indicated by *p* values.

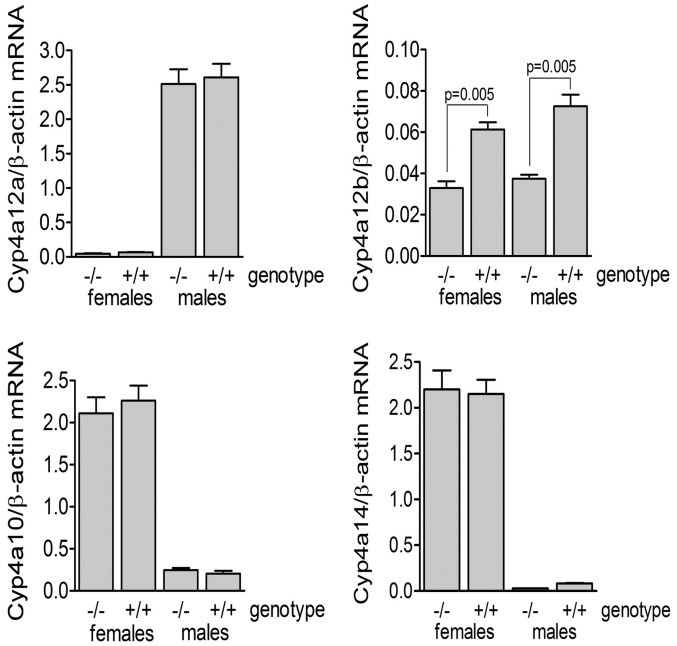

FIGURE 9. **Endogenous renal Cyp4a expression in the absence or presence of the *CYP4A11* transgene.** Quantitative PCR was performed for Cyp4a12a, Cyp4a12b, Cyp4a10, Cyp4a14, and β-actin from reverse transcribed kidney RNA of wild-type (−/−) and B-129/Sv-4A11$^{+/+}$ (+/+). Values represent average Cyp/β-actin mean ratio ± S.E. for each P450 target ($n = 10$ per experimental group). Statistically significant changes are depicted by *p* values.

system in the kidney has the potential to increase sodium uptake (49). Consistent with this possibility, increased AGT mRNA expression was evident in kidneys of B-129/Sv-4A11$^{+/+}$ mice compared with wild-type mice. ACE1 mRNA expression was increased to a lesser extent, and the difference was not statistically significant in male mice. Renin and ATR1 mRNA abundances were not affected by the transgene. The elevation of kidney AGT expression in B-129/Sv-4A11$^{+/+}$ suggested that ANGII (which is produced from AGT in the lumen of the renal tubules) could induce NCC expression. Consistent with this notion, the ATR1 antagonist losartan normalized BP in the B-129/Sv-4A11$^{+/+}$ mice, and the CYP4A11 inhibitor HET0016 reduced renal AGT mRNA expression without affecting BP of wild-type mice. These treatments also restored normal levels of NCC protein, as well as AGT and SGK1 mRNA expression. As elevated kidney-specific expression of an *AGT* transgene led to salt-sensitive hypertension (50), it seems likely that increased AGT synthesis could underlie the effects of the *CYP4A11* transgene on renal sodium homeostasis.

As 20-HETE was elevated in kidney extracts and in urine of B-129/Sv-4A11$^{+/+}$ mice, the 20-HETE antagonists 20-5,16-HEDGE and AAA were employed to examine the role of 20-HETE in the observed hypertensive phenotype. Treatment of B-129/Sv-4A11$^{+/+}$ mice with either antagonist normalized BP and reversed the increases seen for renal AGT, SGK1, and NCC. A large body of evidence indicates that 20-HETE promotes vascular resistance, which could contribute to the observed hypertension (5, 6). Our results do not rule out potential indirect effects of the *CYP4A11* transgene on vascular resistance. Even though plasma 20-HETE concentrations were unaltered in B-129/Sv-4A11$^{+/+}$ mice, elevated luminal 20-HETE could diffuse across the macula densa and accentuate constriction of the afferent arteriole (51, 52). Antagonism of 20-HETE actions in the afferent arteriole could also contribute to the reduction of BP by 20-5,16-HEDGE and AAA. However, the reduction of AGT expression and normalization of NCC and SGK1 expression elicited by the 20-HETE antagonists suggests that these antagonists act more broadly than vascular endothelium and smooth muscle to limit the effects of 20-HETE in epithelial cells. Moreover, these results indicate that the elevation of renal AGT is likely to reflect increased 20-HETE production. The proximal tubule is the predominant site for renal AGT production (53) as well as CYP4A11 expression (1, 17), where 20-HETE could act in an autocrine fashion.

The results of this study contribute to emerging evidence that 20-HETE activates the renin-angiotensin system. This observation was first reported for rats with targeted expression

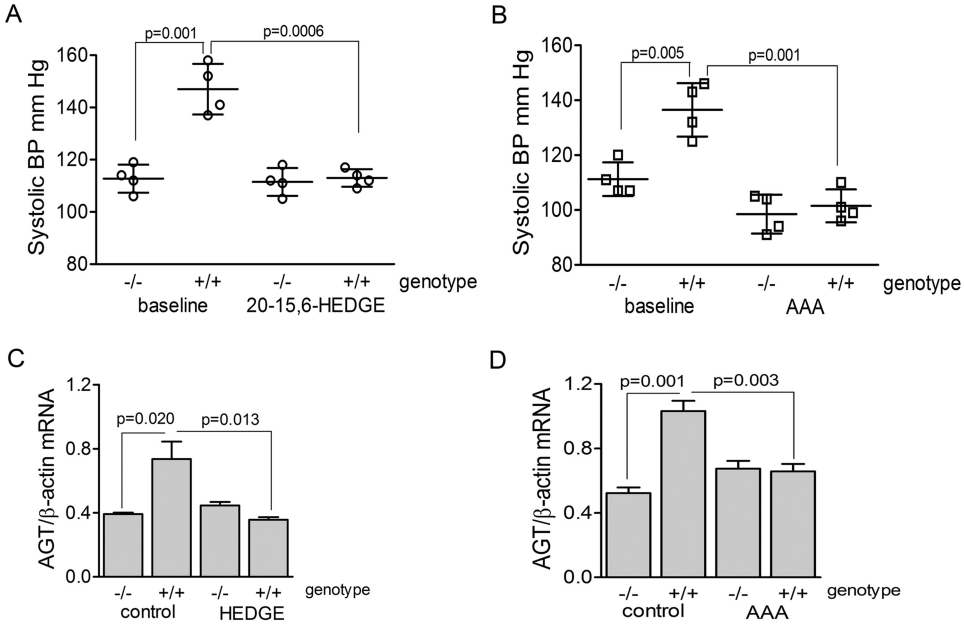

FIGURE 10. **20-HETE antagonists normalize hypertension in B-129/Sv-4A11$^{+/+}$ and attenuate angiotensinogen mRNA increases.** *A*, after baseline BP recordings in females (*circles*), mice were injected with 20-6,15-HEDGE daily and BP recorded on days 7 through 9 while on the compound. *B*, males (*squares*) were given daily injection of AAA and BP was recorded on days 7 through 9. Each *circle* or *square* represents average systolic BP values for each mouse with ±S.D. reflecting the variation within each experimental group. Statistical significance for the effect of each compound on genotype is indicated by the *p* values ($n = 4$ per experimental group). Mean kidney angiotensinogen/β-actin mRNA measurements ±S.E. are shown for mice that were administered 20-6,15-HEDGE (*C*) or AAA (*D*). Statistically significant changes are depicted by *p* values ($n = 4$ per experimental group).

of CYP4A2 in endothelial cells (25). The presence of the transgene increased BP, ACE1, ATR1, and ANGII levels, and the hypertension was normalized by losartan, HET0016, 20-6,15-HEDE, and the ACE1 inhibitor lisinopril. Administration of 20-HETE to cultured endothelial cells was shown to induce expression of ACE1. The modest elevation of ACE1 expression observed in our studies could also be attributed to effects of increased renal production of 20-HETE on endothelial cell ACE1 expression in B-129/Sv-4A11$^{+/+}$ mice. Activation of nuclear factor κ-light chain enhancer of activated B cells (NFκB) is thought to underlie this response to 20-HETE (54), and activation of NFκB has been shown to increase transcription of the *AGT* gene in hepatocytes (55) and renal proximal tubular cells (56), consistent with the notion that 20-HETE activation of NFκB underlies both the elevation of ACE1 and AGT expression. Because losartan normalized SGK1 expression in B-129/Sv-4A11$^{+/+}$ mice, activation of ATR1 is likely to contribute to the elevated expression of SGK1 in kidneys from B-129/Sv-4A11$^{+/+}$ mice, as observed previously for fibroblasts (41, 42). Induction of SGK1 by aldosterone has been shown to contribute to the activation of NCC through a WNK4-mediated pathway (57). However, we have not excluded more direct actions of 20-HETE on this process.

CYP4A11 genetic variants rs3890011 (19) and rs1126742 (12) have been associated with salt-sensitive hypertension in human cohorts. The F434S variant (rs1126742) exhibits 30% lower catalytic efficiency (k_{cat}/K_m) for 20-HETE formation from arachidonic acid *in vitro* than the major allele (12), and the association of the F434S variant with salt-sensitive hypertension has often been interpreted as an effect of reduced CYP4A11 function. The impact of these relative small changes in catalytic efficiency of the F434S variant might be offset by changes in expression of the enzyme due to effects of this or other genetic differences that are in linkage disequilibrium with the F434S mutation, and to date, the effects of genetic variation on CYP4A11 protein expression and activity *in vivo* have not been reported. Interestingly, the V433M variant (rs2108622) of CYP4F2, another human enzyme that catalyzes the ω-hydroxylation of arachidonic acid, also exhibits a reduced k_{cat} *in vitro* (58). Paradoxically, the expression of this V433M allelic variant in human liver has been shown to be much lower than that of the major allelic variant (59, 60), but carriers of the CYP4F2 V433M allele exhibited elevated urinary 20-HETE (61). Hypothetically, loss of CYP4F2 activity could trigger an increase in the compensatory expression of CYP4A11 due to an increased accumulation of free fatty acids that activate peroxisome proliferator-activated receptor α, a transcriptional regulator of CYP4A11 expression (20). SNPs in intron 1 of *CYP4F2* have also been associated with elevated BP and urinary 20-HETE, and the SNPs have been linked to increased *CYP4F2* gene transcription (62). Our studies in B-129/Sv-4A11$^{+/+}$ mice indicate that elevation of kidney 20-HETE production can be associated with salt-sensitive hypertension and changes in water and electrolyte balance, supporting the notion that elevated formation of 20-HETE in humans could contribute to the development of salt-sensitive hypertension. Moreover, our results suggest an increased scope of action for 20-HETE antagonists in the control of hypertension.

Experimental Procedures

Animals—All experiments using mice were conducted with approved protocols by the Institutional Animal Care and Use Committee of The Scripps Research Institute and in accordance with the NIH Guide for the Care and Use of Laboratory

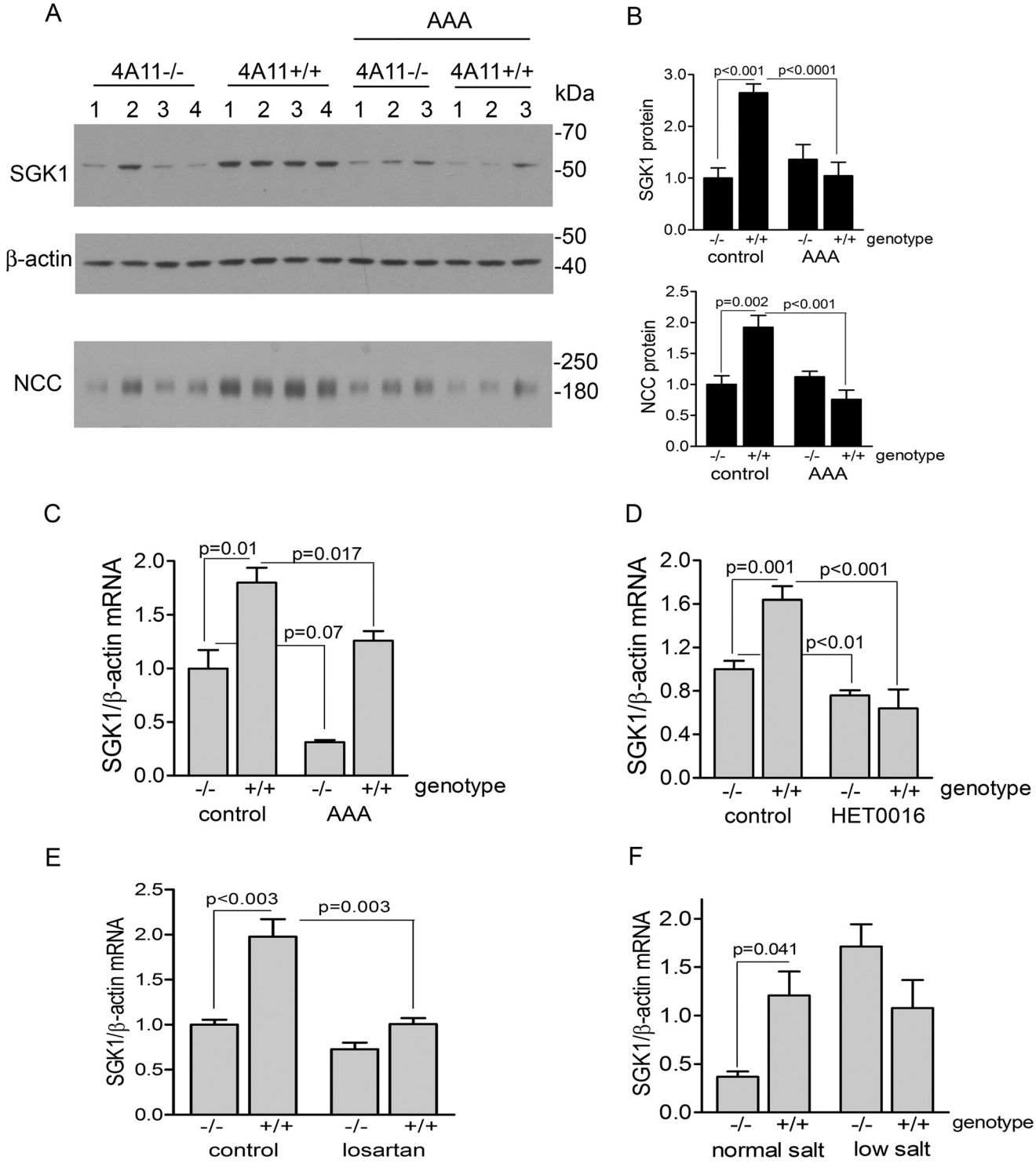

FIGURE 11. **Elevated *SGK1* mRNA expression in B-129/Sv-4A11$^{+/+}$ mice is normalized by the 20-HETE antagonist AAA, HET0016, or losartan.** *A*, kidney homogenates from 10,000 × *g* supernatants (10 μg per lane) of female wild-type (4A11$^{-/-}$) or B-129/Sv-4A11$^{+/+}$ (4A11$^{+/+}$) mice in the absence or presence of 20-HETE antagonist AAA were subjected to immunoblotting using antibodies to SGK1 or β-actin. The membranes were stripped and immunoblotted with the NCC antibody. *B*, quantitation of SGK1 and NCC proteins. The ratios of SGK1/β-actin or NCC/β-actin signals are shown in the bar graphs in the absence (control) or after treatment with AAA. Values represent mean ratios ± S.E. of SGK1/β-actin or NCC/β-actin ratios for control −/−, $n = 7$; control +/+, $n = 7$; AAA −/−, $n = 6$; AAA +/+, $n = 6$. *C*, renal SGK1/β-actin mRNA levels determined by qPCR in female mice in the absence (*control*) or presence of AAA ($n = 4$ per experimental group). *D*, females in the absence (control) or presence of HET0016 ($n = 4$ per experimental group). *E*, females in the absence (control) or presence of losartan ($n = 4$ per experimental group). *F*, SGK1/β-actin mRNA levels in male mice that were given a normal salt or low salt diet ($n = 4$ per experimental group). Statistically significant changes are indicated by the *p* values.

animals. Experiments were generally conducted on groups of male or female 129S6/SvEv Taconic mice (referred to as wild-type or controls) and congenic heterozygous and homozygous *CYP4A11* transgenic mice in the 129/SvEv background. The breeding colony for 129S6/SvEv was established from mice purchased from Taconic. Hemizygous line B and line F transgenic

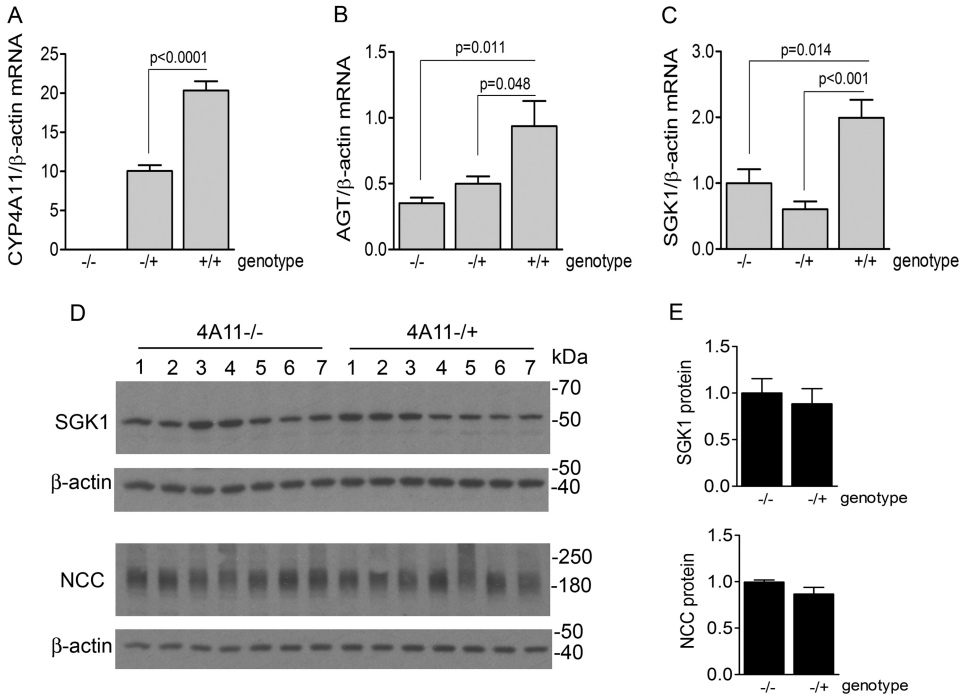

FIGURE 12. *A*, CYP4A11; *B*, AGT; *C*, SGK1 and β-actin mRNA levels in kidney were measured for male wild-type (−/−), heterozygous B-129/Sv-4A11$^{-/+}$ (−/+), and homozygous B-129/Sv-4A11$^{+/+}$ (+/+) mice by qPCR. Values represent mean ± S.E. target/β-actin mRNA ratios for seven biological replicates per group. Statistically significant changes are depicted by the *p* values. *D*, kidney homogenates from 10,000 × *g* supernatants (10 μg/lane) of male wild-type (4A11$^{-/-}$) and heterozygous B-129/Sv-4A11$^{-/+}$ (4A11$^{-/+}$) mice were subjected to immunoblotting using antibodies to SGK1, NCC, or β-actin. Numbers *1–7* depict biological replicates in each group. *E*, target and β-actin protein signals were quantified and are shown as mean ± S.E. for SGK1/β-actin and NCC/β-ratios in the adjacent bar graphs. Statistically significant changes for the −/− *versus* −/+ genotype were not seen ($p > 0.05$).

mice having a tandem repeat with two copies and one copy of the *CYP4A11* gene, respectively, were generated previously in C57Bl/6-Balbc F1 mice (20). Hemizygous congenic line B (B-129/Sv-4A11$^{+/-}$) and line F mice (F-129/Sv-4A11$^{+/-}$) were generated by 9 or more generations of backcrosses of hemizygous line B with 129S6/SvEv mice. After 10 or more generations, two pairs of hemizygous congenic line B mice were mated to produce homozygous line B mice with a total of 4 copies of the CYP4A11 gene. The homozygous line B mice (B-129/Sv-4A11$^{+/+}$) were identified using a gene copy number assay described below. Two pairs of B-129/Sv-4A11$^{+/+}$ mice were used to generate B-129/Sv-4A11$^{+/+}$ mice for the initial BP measurements as described in the legend to Fig. 1. For subsequent experiments, B-129/Sv-4A11$^{+/+}$ mice were maintained by inbreeding descendants of one of the two original breeding pairs. BP measurements were performed initially on heterozygous B-129/Sv-4A11$^{+/-}$ mice after backcross generation 9. Subsequently, heterozygous B-129/Sv-4A11$^{+/-}$ were generated by crossing inbred B-129/Sv-4A11$^{+/+}$ with congenic 129S6/SvEv mice to confirm the initial BP measurements. All mice were housed in an animal facility with an alternating 12-h light (7 a.m.-7 p.m.) and 12-h dark cycle and were provided water and standard rodent chow with 0.3% sodium and 5% fat content (Teklad LM-485) *ad libitum* unless indicated otherwise. A low salt diet (Teklad 94268) that contained 0.05% sodium and 5% fat was given to mice for 3 weeks. Mice were 16–22 weeks of age at time of experimentation unless noted otherwise.

Animal Treatments—The selective P450 ω-hydroxylase inhibitor *N*-hydroxy-*N*′-(4-*n*-butyl-2-methylphenyl)formamidine (HET0016, Cayman Chemicals) was administered by intraperitoneal injection of 10 mg/kg/day in saline that contained 10% L-α-phosphatidylcholine (w/v) (27) for 9 consecutive days. The 20-HETE antagonists sodium 20-6,15-HEDGE and AAA were each given by intraperitoneal injections of 10 mg/kg/day in phosphate-buffered saline for 9 consecutive days (27). HCTZ (MP Biomedical) was administered by daily intraperitoneal injections at 2.5 mg/kg/day for 9 days (30). Prior to administration of the ATR1 blocker losartan (Cayman Chemicals), daily water consumption for mice was determined to calculate the necessary dose to be administered in the drinking water. Losartan was given at 10 mg/kg/day in the drinking water (which was prepared daily) for 7 days (27). Similarly, water consumption was determined for mice, and amiloride (Santa Cruz Biotechnology) was then given in drinking water at 2 mg/kg/day (63). Water consumption was not affected by the presence of either compound. At the end of experimentation, mice were euthanized by an overdose of isoflurane, and tissues were harvested, frozen immediately, and stored at −80 °C until further use.

Transgene Copy Number Determination—A single-copy sensitivity qPCR assay was developed to determine gene copy numbers. To generate standard curves for calibration of *CYP4A11* transgene copies, genomic DNA from wild-type mice was spiked with the BAC clone RP11-345m5 DNA to contain known copy numbers of the human *CYP4A11* gene per copy of the mouse haploid genome. The amounts of BAC clone DNA necessary to achieve this were based on (i) the assumption that a haploid content of a mammalian genome consists of 3×10^9 base pairs, (ii) the BAC clone is 1.23×10^5 base pairs in length, and (iii) the use of 1 μg

of genomic DNA. Copy number standards were generated to contain 0.0, 0.1, 0.5, 1.0, 5, and 10 copies of the BAC clone per haploid equivalent of mouse DNA using 0.0, 4.1, 21, 41, 205, and 410 pg of BAC clone DNA/μg of wild-type mouse DNA. Test samples were prepared at 10 ng/μl from genomic DNA of transgenic lines, and 50 ng of each were used for PCR amplification with *CYP4A11* forward (5′-ATGACGTGGCTTCTTCTGGATA) and reverse (5′-TTGTGCTGAAGGTTCCAAAGTG) primers using SSoAdvanced SYBR Green Supermix (Bio-Rad). *Cyp4a14* (forward 5′-AATTGCTGCCAGATCCCACCAG and reverse 5′-AGGTTCAGTGGCTGGTCAGAGTT primers) was amplified from each sample and served as a one-copy control for a haploid genome.

Blood Pressure Determination—BP was determined using a CODA multichannel non-invasive tail-cuff BP measurement system (Kent Scientific) in conscious mice (64). The CODA system utilizes volume-pressure recording technology to detect changes in tail volume that correspond to systolic and diastolic BP and calculates mean arterial pressure. This non-invasive method for BP measurements in mice was recommended by the American Heart Association Council on High Blood Pressure Research (65) and has gained widespread use. All BP measurements were conducted on adult groups of males and females and performed between 10 a.m. and 2 p.m. at ambient temperature. Prior to initiation of measurements, the animal warming platform (CODA, Kent Scientific) was adjusted to setting 4 and animal holders were placed on top to prewarm. Each mouse was then placed into a holder that is designed to fit the mouse comfortably, whereas minimizing movement during measurements. After the cuffs were attached and secured, animals were placed on the platform and allowed for 5–10 min to thermoregulate. The tail temperature was taken with an infrared thermometer and measurement sessions initiated only when tail temperatures reached 32–35 °C. Each session consisted of 5 acclimation cycles and 20 measurement cycles with session parameters set to a 20-s deflation time, 250 mm Hg occlusion pressure, and a tail volume setting of 15. Generally, 20 BP measurements per session per day were conducted for 10 consecutive days and average and standard deviation of systolic BP was calculated for each individual mouse. BP readings that differed by 2 S.D. from the mean were considered outliers and were excluded, final averages and standard deviations were recalculated for each mouse as recommended (64).

Diagnostic Blood and Urine Chemistry—Mice were transferred to new cages at 4 p.m. on the day prior to blood collection. Their food was removed, but mice had unlimited access to water. In the morning, animals were each euthanized with isoflurane inhalation anesthetic via an open drop method. A 1-cc syringe attached to a 26-gauge needle that had been flushed with heparinized saline was used to collect a terminal blood sample via cardiac puncture. An average of 800 μl of blood could be obtained per mouse. Each blood sample was then transferred into a 1-ml green top Microtainer R tube (BD Biosciences), and the tubes were inverted 3–4 times using a rotating platform. Samples were left at room temperature for 1–2 h and then spun for 10 min at 400 $\times$ *g* at 20 °C. The supernatants were recovered, and only plasma from non-hemolyzed blood was sent for determination of blood chemistry parameters by Antech Diagnostic (Irvine, CA). Plasma aldosterone, ANGII, and renin activity were determined by the Hypertension Core Laboratory at the Hypertension and Vascular Research Center, Wake Forest University. Blood samples were collected as recommended by the Wake Forest Hypertension Core Laboratory. For aldosterone measurements, blood was collected in red-top vacutainer tubes. After clotting, serum was collected after centrifugation for 10 min at 400 $\times$ *g* at room temperature. Samples for determination of plasma ANGII and renin activity were each collected in chilled tubes containing EDTA. Additionally, collection tubes for determination of ANGII contained rat renin inhibitor (Anaspec) and additional protease inhibitors to prevent degradation of ANGII. The samples were stored at −80 °C, and shipped on dry ice to the Wake Forest Hypertension Core Laboratory via overnight shipment.

For urine collection, mice (housed two per cage) were placed in multiple metabolic cages and allowed to adapt. Urine samples were collected after animal body weights, and food and water consumption stabilized. The adaptation period generally lasted 2–3 days and was a necessary step to avoid masking of the results by a fasting response that is usually produced when mice are moved to metabolic cages. Collected urine samples were kept refrigerated and shipped to Antech Diagnostics (Irvine, CA) for same day analysis. Urine samples were collected similarly for measurements of 20-HETE and creatinine. A deuterated d2-20-HETE was added to the sample as internal standard for LC/MS quantification prior to freezing for shipment to Vanderbilt University.

20-HETE Determination by Ultra-high Performance Liquid Chromatography-Tandem Mass Spectrometry (UPLC-MS/MS)—Samples for determination of 20-HETE in tissue homogenates, plasma, or urine were treated with glucuronidase (66) prior to acidification and lipid extraction with chloroform: methanol (2:1, v/v). The dried lipid extract from kidneys, plasma, and urine was dissolved in 80% aqueous methanol containing 0.4 M KOH to hydrolyze 20-HETE esters. The mixture was acidified and extracted into diethyl ether. The extracts were purified by SiO2 chromatography using a solvent 49.5% hexane, 50% diethyl ether, and 0.05% acetic acid (v/v) before quantitative analysis by ULPC-negative ESI-MS/MS (negative ion) monitoring of product ions: *m*/*z* 289 originating from *m*/*z* 319 (20-HETE) and *m*/*z* 289 originating from *m*/*z* 321 (d2–20-HETE), respectively, as described (67–69).

Quantitative PCR—Tissue RNA was isolated using the TRIzol reagent (Life Technologies). Reverse transcription and qPCR was conducted as described previously (20) using the SSoAdvanced SYBR Green Supermix (Bio-Rad). Primers used are listed in Table 4.

Immunoblotting—Whole kidneys were homogenized in 0.1 M potassium phosphate buffer (pH 7.4) containing 0.25 M sucrose, 10 mM sodium pyrophosphate, 10 mM sodium orthovanadate, Pierce™ protease inhibitor mixture (Thermo Scientific), and PhosStop phosphatase inhibitor mixture (Roche Applied Science) using a tissue homogenizer (Biospec Products), as instructed by the suppliers. Tissue homogenates were centrifuged for 5 min to remove debris and again for 15 min at 10,000 $\times$ *g*. The supernatants (referred to as 10K supernatant from here on) were recovered for analysis and equal amounts of

TABLE 4
PCR primers

Gene	Sense 5′-3′	Antisense 5′-3′
Cyp4a10	TCCAGTTCTACCTCCACAGGC	CTAGCATCAATCGAATGGAGTC
Cyp4a12a	AGGATTCCACCCTGGAGATCTTTCG	AGTTTGCAGGCACTGTTAGCCTT
Cyp4a12b	AGGATTCCACCCTGGAGATCTTCCA	AGTTGGCAGGCACTGTTGGCCAA
Cyp4a14	AATTGCTGCCAGATCCCACCAG	AGGTTCAGTGGCTGGTCAGAGTT
Agt	CTGCTCCAGGCTTTCGTCTAA	AGAACTGGGTCAGTGGATAAATCC
Agtr1a (ATR-1)	TCTGCTGCTCTCCCGGACTTA	TATGTAACTGTGCCTGCCAGC
Ace-1	CACTATGGGTCCGAGTACAT	ATCATAGATGTTGGACCAGG
Ace-2	TGCCCATTTGCTTGGTGAT	AAAGGGAACAGTCAAAGGGTACAG
Ren-1	AGTCTCCCAACACGCACCGCT	AGTGGATGGTGAAGTCGGACCCG
Ren-2	TCAGTCTCCCAACGGGCACCAC	CGGGTCCGACTTCACCATCCACT
Sgk-1	AACTGGGCAACTGCTTCATC	GCCTTTGTCGGAAAAACATC
11β−Hsd2	AACTGCGTGACCTCTGTTCTCCT	GCACCAAAGAAGTTCACCTCCATG
Slc12a3 (NCC)	CCTCCATCACCAACTCACCT	CCGCCCACTTGCTGTAGTA
β−Actin	GCTGCGTTTTACACCCTTTCTT	AAGTCCTCAGCCACATTTGTAG

protein were separated on SDS-PAGE gels. Proteins were transferred to nitrocellulose and blotted with primary rabbit polyclonal antibody to NCC (AB3553, Millipore) at 1:2000 dilution followed by an anti-rabbit HRP conjugate (Promega) at 1:10,000. Antibodies to NCC phosphorylated at residue Thr-53, Thr-58, Ser-71, or Ser-89, respectively, were generously provided by Dr. Johannes Loffing (University of Zurich, Switzerland) and used on 100,000 × *g* pellets from kidneys (referred to as 100K pellet) as described in a procedure from the Loffing laboratory to assess changes in phosphorylation status (33). The anti-rabbit HRP conjugate at a 1:20,000 dilution served as secondary antibody. Rabbit monoclonal antibody to SGK1 (ab32374, Abcam) was used at a 1:2000 dilution, followed by the anti-rabbit HRP conjugate at a 40,000 dilution to determine SGK1 protein levels. A polyclonal rabbit anti β-actin (NB600–503SS Novus Biologicals) antibody was used as a loading control at a 1:20,000 dilution followed by the anti-rabbit HRP conjugate at 1:20,000. Immunoreactive proteins were visualized by enhanced chemiluminescence (PerkinElmer Life Sciences). Membranes were exposed to Kodak Biomax X-AR autoradiography film (Carestream) and bands were quantified by using the LiCor Image Studio Lite version 4.0 software. For each target, multiple sample amounts were loaded to ensure that the detected signal was within the linear range of exposure.

Statistics—Statistical significance was determined for comparisons of two groups by applying Student's two-tailed *t* test. For comparisons of multiple groups, analysis of variance with the Bonferroni's post test was conducted with the GraphPad Prism software version 5.0 (GraphPad, La Jolla, CA), and *p* values less than 0.05 were considered significant.

Author Contributions—U. S., J. H. C., and E. F. J. designed the study. U. S. and E. F. J. drafted the manuscript. J. H. C., F. P. G., M. H., and S. W. characterized differences in urinary and tissue 20-HETE formation. J. R. F. designed and synthesized the 20-HETE antagonists and advised on their application in this study. U. S. conducted all other experiments. All authors analyzed the results, contributed to writing the manuscript, and approved the final version of the manuscript.

Acknowledgments—We thank Dr. Johannes Loffing (University of Zurich) for his generous gift of antibodies to pT53-NCC, pT58-NCC, pS71-NCC, and pS89-NCC and thank Tho Ta (Scripps) for technical assistance with breeding the mouse strains used in this study.

References

1. Lasker, J. M., Chen, W. B., Wolf, I., Bloswick, B. P., Wilson, P. D., and Powell, P. K. (2000) Formation of 20-hydroxyeicosatetraenoic acid, a vasoactive and natriuretic eicosanoid, in human kidney: role of Cyp4F2 and Cyp4A11. *J. Biol. Chem.* **275,** 4118–4126
2. Powell, P. K., Wolf, I., Jin, R., and Lasker, J. M. (1998) Metabolism of arachidonic acid to 20-hydroxy-5,8,11,14- eicosatetraenoic acid by P450 enzymes in human liver: involvement of CYP4F2 and CYP4A11. *J. Pharmacol. Exp. Ther.* **285,** 1327–1336
3. Powell, P. K., Wolf, I., and Lasker, J. M. (1996) Identification of CYP4A11 as the major lauric acid ω- hydroxylase in human liver microsomes. *Arch. Biochem. Biophys.* **335,** 219–226
4. Capdevila, J. H., Wang, W., and Falck, J. R. (2015) Arachidonic acid monooxygenase: genetic and biochemical approaches to physiological/pathophysiological relevance. *Prostaglandins Other Lipid Mediat.* **120,** 40–49
5. Fan, F., Muroya, Y., and Roman, R. J. (2015) Cytochrome P450 eicosanoids in hypertension and renal disease. *Curr. Opin. Nephrol. Hypertens.* **24,** 37–46
6. Wu, C. C., Gupta, T., Garcia, V., Ding, Y., and Schwartzman, M. L. (2014) 20-HETE and blood pressure regulation: clinical implications. *Cardiol. Rev.* **22,** 1–12
7. Gainer, J. V., Bellamine, A., Dawson, E. P., Womble, K. E., Grant, S. W., Wang, Y., Cupples, L. A., Guo, C. Y., Demissie, S., O'Donnell, C. J., Brown, N. J., Waterman, M. R., and Capdevila, J. H. (2005) Functional variant of CYP4A11 20-Hydroxyeicosatetraenoic acid synthase is associated with essential hypertension. *Circulation* **111,** 63–69
8. Sugimoto, K., Akasaka, H., Katsuya, T., Node, K., Fujisawa, T., Shimaoka, I., Yasuda, O., Ohishi, M., Ogihara, T., Shimamoto, K., and Rakugi, H. (2008) A polymorphism regulates CYP4A11 transcriptional activity and is associated with hypertension in a Japanese population. *Hypertension* **52,** 1142–1148
9. Mayer, B., Lieb, W., Götz, A., König, I. R., Aherrahrou, Z., Thiemig, A., Holmer, S., Hengstenberg, C., Doering, A., Loewel, H., Hense, H. W., Schunkert, H., and Erdmann, J. (2005) Association of the T8590C polymorphism of CYP4A11 with hypertension in the MONICA Augsburg echocardiographic substudy. *Hypertension* **46,** 766–771
10. Mayer, B., Lieb, W., Götz, A., König, I. R., Kauschen, L. F., Linsel-Nitschke, P., Pomarino, A., Holmer, S., Hengstenberg, C., Doering, A., Loewel, H., Hense, H. W., Ziegler, A., Erdmann, J., and Schunkert, H. (2006) Association of a functional polymorphism in the CYP4A11 gene with systolic blood pressure in survivors of myocardial infarction. *J. Hypertens.* **24,** 1965–1970
11. Gainer, J. V., Lipkowitz, M. S., Yu, C., Waterman, M. R., Dawson, E. P., Capdevila, J. H., Brown, N. J., and AASK Study Group (2008) Association of a CYP4A11 variant and blood pressure in black men. *J. Am. Soc. Nephrol.* **19,** 1606–1612
12. Laffer, C. L., Gainer, J. V., Waterman, M. R., Capdevila, J. H., Laniado-Schwartzman, M., Nasjletti, A., Brown, N. J., and Elijovich, F. (2008) The T8590C polymorphism of CYP4A11 and 20-hydroxyeicosatetraenoic acid in essential hypertension. *Hypertension* **51,** 767–772

13. Hermann, M., Hellermann, J. P., Quitzau, K., Hoffmann, M. M., Gasser, T., Meinertz, T., Münzel, T., Fleming, I., and Lüscher, T. F. (2009) CYP4A11 polymorphism correlates with coronary endothelial dysfunction in patients with coronary artery disease: the ENCORE Trials. *Atherosclerosis* **207,** 476–479
14. Zhang, R., Lu, J., Hu, C., Wang, C., Yu, W., Ma, X., Bao, Y., Xiang, K., Guan, Y., and Jia, W. (2011) A common polymorphism of CYP4A11 is associated with blood pressure in a Chinese population. *Hypertens. Res.* **34,** 645–648
15. Yang, H., Fu, Z., Ma, Y., Huang, D., Zhu, Q., Erdenbat, C., Xie, X., Liu, F., and Zheng, Y. (2014) CYP4A11 gene T8590C polymorphism is associated with essential hypertension in the male Western Chinese Han population. *Clin. Exp. Hypertens.* **36,** 398–403
16. Zhang, C., Wang, L., Liao, Q., Zhang, L., Xu, L., Chen, C., Ye, H., Xu, X., Ye, M., and Duan, S. (2013) Genetic associations with hypertension: meta-analyses of six candidate genetic variants. *Genet. Test. Mol. Biomarkers* **17,** 736–742
17. Ito, O., Nakamura, Y., Tan, L., Ishizuka, T., Sasaki, Y., Minami, N., Kanazawa, M., Ito, S., Sasano, H., and Kohzuki, M. (2006) Expression of cytochrome P-450 4 enzymes in the kidney and liver: Regulation by PPAR and species-difference between rat and human. *Mol. Cell. Biochem.* **284,** 141–148
18. Williams, J. S., Hopkins, P. N., Jeunemaitre, X., and Brown, N. J. (2011) CYP4A11 T8590C polymorphism, salt-sensitive hypertension, and renal blood flow. *J. Hypertens.* **29,** 1913–1918
19. Laffer, C. L., Elijovich, F., Eckert, G. J., Tu, W., Pratt, J. H., and Brown, N. J. (2014) Genetic variation in CYP4A11 and blood pressure response to mineralocorticoid receptor antagonism or ENaC inhibition: an exploratory pilot study in African Americans. *J. Am. Soc. Hypertens.* **8,** 475–480
20. Savas, U., Machemer, D. E., Hsu, M. H., Gaynor, P., Lasker, J. M., Tukey, R. H., and Johnson, E. F. (2009) Opposing roles of peroxisome proliferator-activated receptor alpha and growth hormone in the regulation of CYP4A11 expression in a transgenic mouse model. *J. Biol. Chem.* **284,** 16541–16552
21. Uhlén, M., Fagerberg, L., Hallström, B. M., Lindskog, C., Oksvold, P., Mardinoglu, A., Sivertsson, A., Kampf, C., Sjöstedt, E., Asplund, A., Olsson, I., Edlund, K., Lundberg, E., Navani, S., Szigyarto, C. A., *et al.* (2015) Proteomics: tissue-based map of the human proteome. *Science* **347,** 1260419
22. Holla, V. R., Adas, F., Imig, J. D., Zhao, X., Price, E., Jr., Olsen, N., Kovacs, W. J., Magnuson, M. A., Keeney, D. S., Breyer, M. D., Falck, J. R., Waterman, M. R., and Capdevila, J. H. (2001) Alterations in the regulation of androgen-sensitive Cyp4a monooxygenases cause hypertension. *Proc. Natl. Acad. Sci. U.S.A.* **98,** 5211–5216
23. Liu, X., Zhao, Y., Wang, L., Yang, X., Zheng, Z., Zhang, Y., Chen, F., and Liu, H. (2009) Overexpression of cytochrome P450 4F2 in mice increases 20-hydroxyeicosatetraenoic acid production and arterial blood pressure. *Kidney Int.* **75,** 1288–1296
24. Liu, X., Wu, J., Liu, H., Lai, G., and Zhao, Y. (2012) Disturbed ratio of renal 20-HETE/EETs is involved in androgen-induced hypertension in cytochrome P450 4F2 transgenic mice. *Gene* **505,** 352–359
25. Sodhi, K., Wu, C. C., Cheng, J., Gotlinger, K., Inoue, K., Goli, M., Falck, J. R., Abraham, N. G., and Schwartzman, M. L. (2010) CYP4A2-induced hypertension is 20-hydroxyeicosatetraenoic acid- and angiotensin II-dependent. *Hypertension* **56,** 871–878
26. Cheng, J., Garcia, V., Ding, Y., Wu, C. C., Thakar, K., Falck, J. R., Ramu, E., and Schwartzman, M. L. (2012) Induction of angiotensin-converting enzyme and activation of the renin-angiotensin system contribute to 20-hydroxyeicosatetraenoic acid-mediated endothelial dysfunction. *Arterioscler. Thromb. Vasc. Biol.* **32,** 1917–1924
27. Wu, C. C., Mei, S., Cheng, J., Ding, Y., Weidenhammer, A., Garcia, V., Zhang, F., Gotlinger, K., Manthati, V. L., Falck, J. R., Capdevila, J. H., and Schwartzman, M. L. (2013) Androgen-sensitive hypertension associates with upregulated vascular CYP4A12-20-HETE synthase. *J. Am. Soc. Nephrol.* **24,** 1288–1296
28. Miyata, N., Taniguchi, K., Seki, T., Ishimoto, T., Sato-Watanabe, M., Yasuda, Y., Doi, M., Kametani, S., Tomishima, Y., Ueki, T., Sato, M., and Kameo, K. (2001) HET0016, a potent and selective inhibitor of 20-HETE synthesizing enzyme. *Br. J. Pharmacol.* **133,** 325–329
29. Edson, K. Z., and Rettie, A. E. (2013) CYP4 enzymes as potential drug targets: focus on enzyme multiplicity, inducers and inhibitors, and therapeutic modulation of 20-hydroxyeicosatetraenoic acid (20-HETE) synthase and fatty acid ω-hydroxylase activities. *Curr. Top. Med. Chem.* **13,** 1429–1440
30. Yang, S. S., Morimoto, T., Rai, T., Chiga, M., Sohara, E., Ohno, M., Uchida, K., Lin, S. H., Moriguchi, T., Shibuya, H., Kondo, Y., Sasaki, S., and Uchida, S. (2007) Molecular pathogenesis of pseudohypoaldosteronism type II: generation and analysis of a Wnk4(D561A/+) knockin mouse model. *Cell Metab.* **5,** 331–344
31. Pacheco-Alvarez, D., Cristóbal, P. S., Meade, P., Moreno, E., Vazquez, N., Muñoz, E., Díaz, A., Juárez, M. E., Giménez, I., and Gamba, G. (2006) The Na^+:Cl^- cotransporter is activated and phosphorylated at the amino-terminal domain upon intracellular chloride depletion. *J. Biol. Chem.* **281,** 28755–28763
32. Glover, M., Zuber, A. M., and O'Shaughnessy, K. M. (2009) Renal and brain isoforms of WNK3 have opposite effects on NCCT expression. *J. Am. Soc. Nephrol.* **20,** 1314–1322
33. Sorensen, M. V., Grossmann, S., Roesinger, M., Gresko, N., Todkar, A. P., Barmettler, G., Ziegler, U., Odermatt, A., Loffing-Cueni, D., and Loffing, J. (2013) Rapid dephosphorylation of the renal sodium chloride cotransporter in response to oral potassium intake in mice. *Kidney Int.* **83,** 811–824
34. Sandberg, M. B., Riquier, A. D., Pihakaski-Maunsbach, K., McDonough, A. A., and Maunsbach, A. B. (2007) ANG II provokes acute trafficking of distal tubule Na^+-Cl^- cotransporter to apical membrane. *Am. J. Physiol. Renal Physiol.* **293,** F662–669
35. van der Lubbe, N., Lim, C. H., Fenton, R. A., Meima, M. E., Jan Danser, A. H., Zietse, R., and Hoorn, E. J. (2011) Angiotensin II induces phosphorylation of the thiazide-sensitive sodium chloride cotransporter independent of aldosterone. *Kidney Int.* **79,** 66–76
36. Navar, L. G. (2013) Translational studies on augmentation of intratubular renin-angiotensin system in hypertension. *Kidney Int. Suppl.* **3,** 321–325
37. Craigie, E., Evans, L. C., Mullins, J. J., and Bailey, M. A. (2012) Failure to downregulate the epithelial sodium channel causes salt sensitivity in Hsd11b2 heterozygote mice. *Hypertension* **60,** 684–690
38. Alonso-Galicia, M., Falck, J. R., Reddy, K. M., and Roman, R. J. (1999) 20-HETE agonists and antagonists in the renal circulation. *Am. J. Physiol.* **277,** F790–F796
39. Garcia, V., Cheng, J., Weidenhammer, A., Ding, Y., Wu, C. C., Zhang, F., Gotlinger, K., Falck, J. R., and Schwartzman, M. L. (2015) Androgen-induced hypertension in angiotensinogen deficient mice: role of 20-HETE and EETS. *Prostaglandins Other Lipid Mediat.* **116–117**, 124–130
40. Lang, F., and Shumilina, E. (2013) Regulation of ion channels by the serum- and glucocorticoid-inducible kinase SGK1. *FASEB J.* **27,** 3–12
41. Hussain, A., Wyatt, A. W., Wang, K., Bhandaru, M., Biswas, R., Avram, D., Föller, M., Rexhepaj, R., Friedrich, B., Ullrich, S., Müller, G., Kuhl, D., Risler, T., and Lang, F. (2008) SGK1-dependent upregulation of connective tissue growth factor by angiotensin II. *Kidney Blood Press. Res.* **31,** 80–86
42. Baskin, R., and Sayeski, P. P. (2012) Angiotensin II mediates cell survival through upregulation and activation of the serum and glucocorticoid inducible kinase 1. *Cell. Signal.* **24,** 435–442
43. Stevens, V. A., Saad, S., Poronnik, P., Fenton-Lee, C. A., Polhill, T. S., and Pollock, C. A. (2008) The role of SGK-1 in angiotensin II-mediated sodium reabsorption in human proximal tubular cells. *Nephrol. Dial. Transplant.* **23,** 1834–1843
44. Fan, X., Liu, K., Cui, W., Huang, J., Wang, W., and Gao, Y. (2014) Novel mechanism of intrarenal angiotensin II-induced sodium/proton exchanger 3 expression by losartan in spontaneously hypertensive rats. *Mol. Med. Rep.* **10,** 2483–2488
45. O'Shaughnessy, K. M. (2015) Gordon syndrome: a continuing story. *Pediatr. Nephrol.* **30,** 1903–1908
46. Quigley, R., Chakravarty, S., Zhao, X., Imig, J. D., and Capdevila, J. H. (2009) Increased renal proximal convoluted tubule transport contributes to hypertension in Cyp4a14 knockout mice. *Nephron Physiol.* **113,** 23–28
47. Wu, J., Liu, X., Lai, G., Yang, X., Wang, L., and Zhao, Y. (2013) Synergistical effect of 20-HETE and high salt on NKCC2 protein and blood pres-

sure via ubiquitin-proteasome pathway. *Hum. Genet.* **132,** 179–187
48. van der Lubbe, N., Zietse, R., and Hoorn, E. J. (2013) Effects of angiotensin II on kinase-mediated sodium and potassium transport in the distal nephron. *Curr. Opin. Nephrol. Hypertens.* **22,** 120–126
49. Sparks, M. A., Crowley, S. D., Gurley, S. B., Mirotsou, M., and Coffman, T. M. (2014) Classical renin-angiotensin system in kidney physiology. *Compr. Physiol.* **4,** 1201–1228
50. Ying, J., Stuart, D., Hillas, E., Gociman, B. R., Ramkumar, N., Lalouel, J. M., and Kohan, D. E. (2012) Overexpression of mouse angiotensinogen in renal proximal tubule causes salt-sensitive hypertension in mice. *Am. J. Hypertens.* **25,** 684–689
51. Zou, A.-I., Imig, J. D., Ortiz de Montellano, P. R., Sui, Z., Falck, J. R., and Roman, R. J. (1994) Effect of *P*-450 omega-hydroxylase metabolites of arachidonic acid on tubuloglomerular feedback. *Am. J. Physiol.* **266,** F934–F941
52. Ge, Y., Murphy, S. R., Lu, Y., Falck, J., Liu, R., and Roman, R. J. (2013) Endogenously produced 20-HETE modulates myogenic and TGF response in microperfused afferent arterioles. *Prostaglandins Other Lipid Mediat.* **102–103**, 42–48
53. Rohrwasser, A., Morgan, T., Dillon, H. F., Zhao, L., Callaway, C. W., Hillas, E., Zhang, S., Cheng, T., Inagami, T., Ward, K., Terreros, D. A., and Lalouel, J. M. (1999) Elements of a paracrine tubular renin-angiotensin system along the entire nephron. *Hypertension* **34,** 1265–1274
54. Garcia, V., Shkolnik, B., Milhau, L., Falck, J. R., and Schwartzman, M. L. (2016) 20-HETE activates the transcription of angiotensin converting enzyme (ACE) via NF-κB translocation and promoter binding. *J. Pharmacol. Exp. Ther.* **356,** 525–533
55. Brasier, A. R., Li, J., and Copland, A. (1994) Transcription factors modulating angiotensinogen gene expression in hepatocytes. *Kidney Int.* **46,** 1564–1566
56. Acres, O. W., Satou, R., Navar, L. G., and Kobori, H. (2011) Contribution of a nuclear factor-κB binding site to human angiotensinogen promoter activity in renal proximal tubular cells. *Hypertension* **57,** 608–613
57. Rozansky, D. J., Cornwall, T., Subramanya, A. R., Rogers, S., Yang, Y. F., David, L. L., Zhu, X., Yang, C. L., and Ellison, D. H. (2009) Aldosterone mediates activation of the thiazide-sensitive Na-Cl cotransporter through an SGK1 and WNK4 signaling pathway. *J. Clin. Invest.* **119,** 2601–2612
58. Stec, D. E., Roman, R. J., Flasch, A., and Rieder, M. J. (2007) A functional polymorphism in human CYP4F2 decreases 20-HETE production. *Physiol. Genomics* **30,** 74–81
59. McDonald, M. G., Rieder, M. J., Nakano, M., Hsia, C. K., and Rettie, A. E. (2009) CYP4F2 is a vitamin K1 oxidase: an explanation for altered warfarin dose in carriers of the V433M variant. *Mol. Pharmacol.* **75,** 1337–1346
60. Edson, K. Z., Prasad, B., Unadkat, J. D., Suhara, Y., Okano, T., Guengerich, F. P., and Rettie, A. E. (2013) Cytochrome P450-dependent catabolism of vitamin K: ω-hydroxylation catalyzed by human CYP4F2 and CYP4F11. *Biochemistry* **52,** 8276–8285
61. Ward, N. C., Tsai, I. J., Barden, A., van Bockxmeer, F. M., Puddey, I. B., Hodgson, J. M., and Croft, K. D. (2008) A single nucleotide polymorphism in the CYP4F2 but not CYP4A11 gene is associated with increased 20-HETE excretion and blood pressure. *Hypertension* **51,** 1393–1398
62. Liu, H., Zhao, Y., Nie, D., Shi, J., Fu, L., Li, Y., Yu, D., and Lu, J. (2008) Association of a functional cytochrome P450 4F2 haplotype with urinary 20-HETE and hypertension. *J. Am. Soc. Nephrol.* **19,** 714–721
63. Nakagawa, K., Holla, V. R., Wei, Y., Wang, W. H., Gatica, A., Wei, S., Mei, S., Miller, C. M., Cha, D. R., Price, E., Jr., Zent, R., Pozzi, A., Breyer, M. D., Guan, Y., Falck, J. R., Waterman, M. R., and Capdevila, J. H. (2006) Salt-sensitive hypertension is associated with dysfunctional *Cyp4a10* gene and kidney epithelial sodium channel. *J. Clin. Invest.* **116,** 1696–1702
64. Feng, M., Whitesall, S., Zhang, Y., Beibel, M., D'Alecy, L., and DiPetrillo, K. (2008) Validation of volume-pressure recording tail-cuff blood pressure measurements. *Am. J. Hypertens.* **21,** 1288–1291
65. Kurtz, T. W., Griffin, K. A., Bidani, A. K., Davisson, R. L., Hall, J. E., Subcommittee of Professional and Public Education of the American Heart Association (2005) Recommendations for blood pressure measurement in humans and experimental animals: part 2, blood pressure measurement in experimental animals: a statement for professionals from the subcommittee of professional and public education of the American Heart Association council on high blood pressure research. *Hypertension* **45,** 299–310
66. Prakash, C., Zhang, J. Y., Falck, J. R., Chauhan, K., and Blair, I. A. (1992) 20-Hydroxyeicosatetraenoic acid is excreted as a glucuronide conjugate in human urine. *Biochem. Biophys. Res. Commun.* **185,** 728–733
67. Capdevila, J. H., Falck, J. R., Dishman, E., and Karara, A. (1990) Cytochrome *P*-450 arachidonate oxygenase. *Methods Enzymol.* **187,** 385–394
68. Cowart, L. A., Wei, S., Hsu, M. H., Johnson, E. F., Krishna, M. U., Falck, J. R., and Capdevila, J. H. (2002) The CYP4A isoforms hydroxylate epoxyeicosatrienoic acids to form high affinity peroxisome proliferator-activated receptor ligands. *J. Biol. Chem.* **277,** 35105–35112
69. Capdevila, J. H., Pidkovka, N., Mei, S., Gong, Y., Falck, J. R., Imig, J. D., Harris, R. C., and Wang, W. (2014) The Cyp2c44 epoxygenase regulates epithelial sodium channel activity and the blood pressure responses to increased dietary salt. *J. Biol. Chem.* **289,** 4377–4386